Realistic Phenomenological Nuclear Mean Field Theory: Part [3] Examples of Applications – Nucleonic States in Deformed Nuclei

Jerzy DUDEK

University of Strasbourg/IPHC/CNRS, France
and
The Henryk Niewodniczański Institute of Nuclear Physics
Polish Academy of Sciences, Kraków, Poland

Theo4Exp EUROLABS Hands-on Workshop

Examples of Collaboration Theory-Experiment*)

- **Potential Energy Maps**
- **Isomers in Axial Nuclei**
- **Hartree Fock Bogolyubov Cranking – Back-Bending**
- **Shape-Transition Probabilities**
- **Spatial Distributions of Nucleonic Wave Functions**

– – – – –

*) Based on computer codes already available as well as to be installed

Section 1

Large-Scale Calculations of Nuclear Potential Energies with Multi-Processor Systems

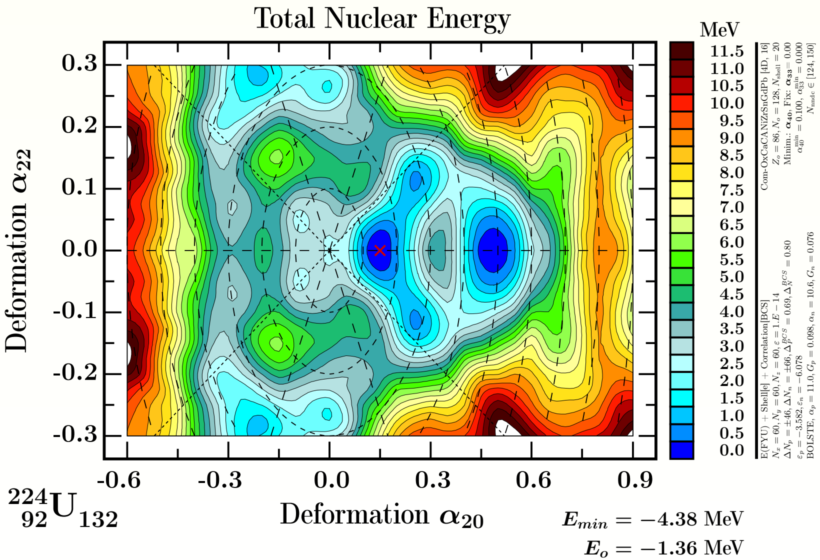

- Here: Energy minimised over α_{40} and α_{33}

Reminder: $(\beta, \gamma) \leftrightarrow \mathcal{O}_{x,y,z}$ - Axis Orientations

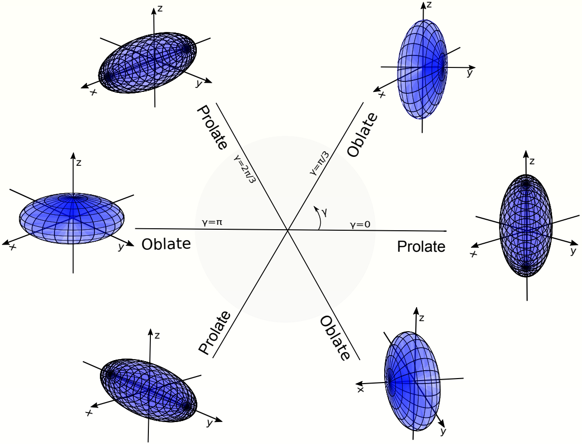

- **We work in multidimensional deformation spaces: ∼3D, 4D, 5D**

Reminder: $(\beta, \gamma) \leftrightarrow \mathcal{O}_{x,y,z}$ - Axis Orientations

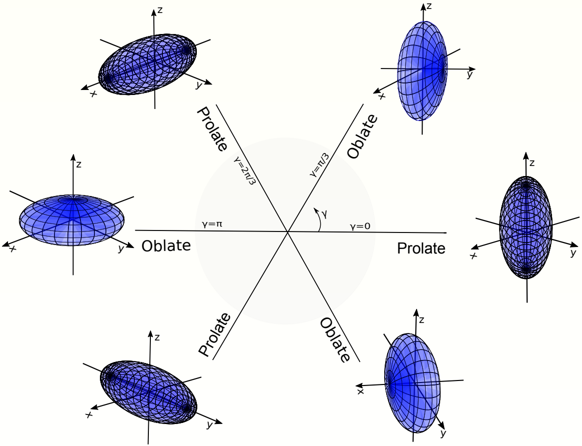

- **We work in multidimensional deformation spaces: ∼3D, 4D, 5D**
  - **We must not use the "camembert $\Delta\gamma = 60^o$ approximation"**

Simultaneous Minimisation over α_{40} and α_{33}

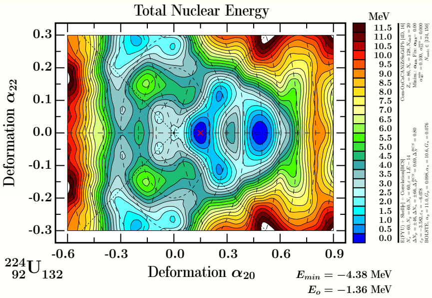

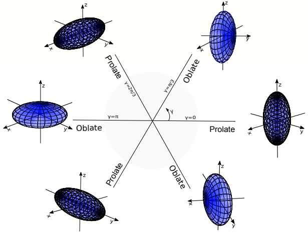

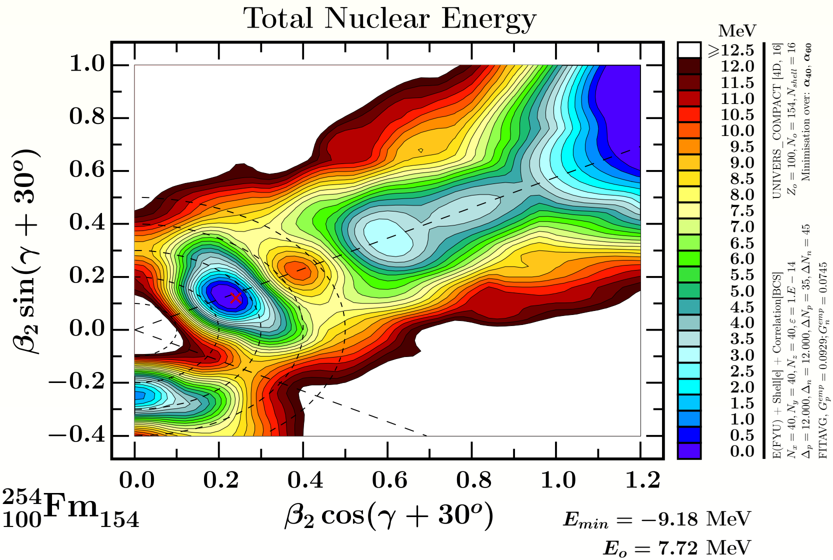

- Here: Energy minimised over α_{40} and α_{60}; NO CAMEMBERS

Example 3 – Tracing Exotic Octupole α_{32} – Tetrahedron

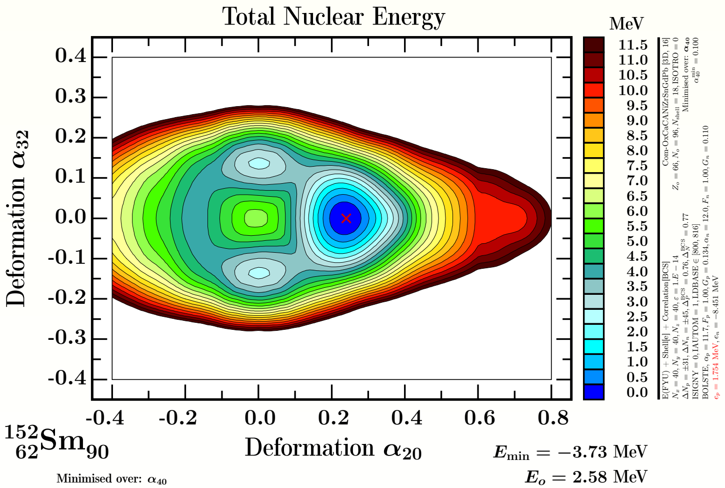

- Example of TETRAHEDRAL SYMMETRY minima.

Prediction confirmed experimentally by JD and SB and collaborators:
Phys. Rev. C 97, 021302(R) (2018) and Phys. Rev. C 111, 034319 (2025)

Example 4: Four Coexisting Octupole Projections

- 2D projections: $(\alpha_{31}, \alpha_{30})$, $(\alpha_{32}, \alpha_{30})$, $(\alpha_{33}, \alpha_{30})$, $(\alpha_{32}, \alpha_{31})$, $(\alpha_{33}, \alpha_{31})$, $(\alpha_{33}, \alpha_{32})$

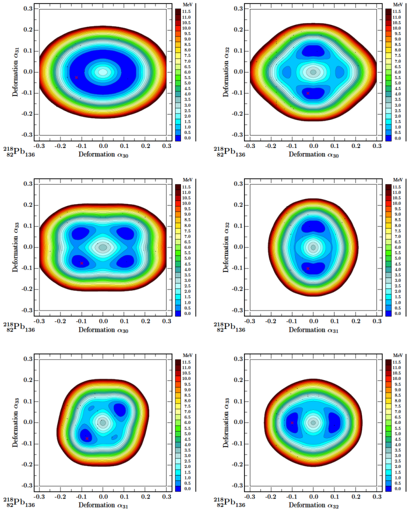

- We should NOT forget that "octupole" is NOT l i m i t e d to "pear shape"

Synthetic Comments For This Part

- **Our nuclear potential data base contains $\underline{\underline{\sim 90\,000 \text{ various projections}}}$ (usually called "maps") for several hundreds of even-even nuclei**
- **We believe, the approach is well adapted to support interpretation of various experiments and new proposal writing**

Section 2

K-Isomers, Yrast Trap Isomers, Axial-Symmetry Imposed Hindrance Factors, and Mean-Field Theory Interpretation

Nuclear Spins Aligned With the Symmetry Axis

• One uses mean-field approach and the fact that in the case of an axial symmetry, say $\mathcal{O}_z$-axis we have

$$\boxed{[\hat{H}, \hat{\jmath}_z] = 0}$$

• Consequently

$$\boxed{\hat{H}\phi_{\nu,m_\nu} = e_{\nu,m_\nu}\phi_{\nu,m_\nu}}$$

$$\boxed{\hat{\jmath}_z\phi_{\nu,m_\nu} = m_\nu\phi_{\nu,m_\nu}}$$

Projections of Angular Momenta Are Conserved in the Presence of Axial Symmetry

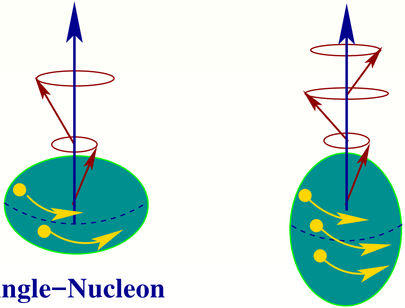

Single−Nucleon Alignment

• The presence of axial symmetry (like any other symmetry) imposes certain hindrance mechanism: In the present case $\rightarrow\rightarrow\rightarrow$ K-isomers

Tilted Fermi Surface: Lagrange Multiplier Method

- We would like to find the lowest energy excited configurations. $\mathcal{C}$, denotes ensemble of indices of occupied states for protons and neutrons separately:

$$E^* = \sum_{\nu \in \{\mathcal{C}\}} e_\nu, \qquad (A)$$

- The number of particles $\mathcal{N}$ – is equal to N or Z

$$\sum_{\nu \in \{C\}} 1_\nu = \mathcal{N}, \qquad (B)$$

- The projected angular momentum, $\mathcal{M}$, corresponds either to proton or to the neutron contributions, M_Z or M_N, respectively

$$\sum_{\nu \in \{C\}} m_\nu = \mathcal{M} \quad (M_Z \text{ or } M_N). \qquad (C)$$

- According to the Lagrange theorem, minimisation of (A) under conditions (B) and (C) is equivalent to the minimisation of an auxiliary expression

$$\boldsymbol{\tilde{E}^*_M = \sum_{\nu \in \{C\}} (e_\nu - \lambda \cdot 1_\nu - \omega \cdot m_\nu), \; (D)}$$

where the so called Lagrange multipliers $\boldsymbol{\lambda}$ and $\boldsymbol{\omega}$ are so far unknown.

Tilted Fermi Surface: Lagrange Multiplier Method

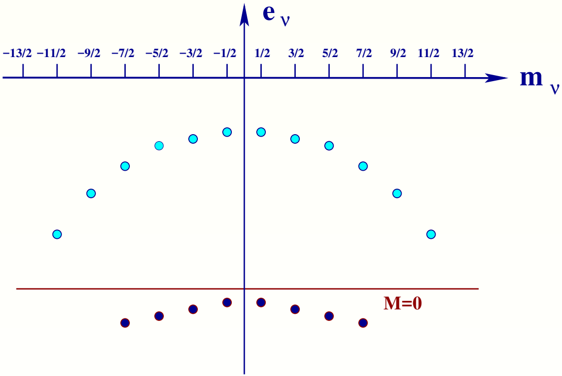

Minimisation of the expression in Eq. (D) under the conditions specified by Eqs. (A-B) is equivalent to searching the lowest points (e_ν, m_ν)

$$\tilde{E}^*_M = \sum_{\nu \in \{C\}} (e_\nu - \lambda \cdot 1_\nu - \omega \cdot m_\nu),$$

equivalent to finding all points strictly below the straight line

$$e = \lambda - \omega m$$

Tilted Fermi Surface: Energy Minimisation at Fixed Spin

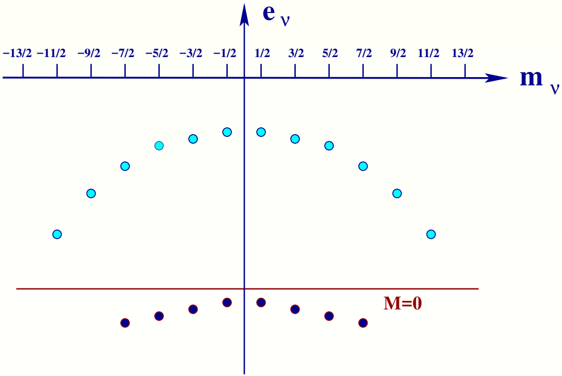

For the **p**article-**h**ole excited-states we obtain at the same time the theoretical energy and theoretical spin $\to\to\to$ A. Bohr hypothesis:

$$\boxed{I \approx M^*}$$

$$E^* = \sum_p e_{p,m_p} - \sum_h e_{h,m_h} \quad \text{and} \quad I \approx M^* = \sum_p m_p - \sum_h m_h$$

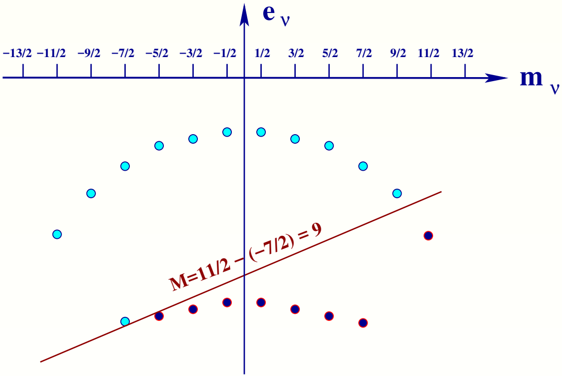

For the **p**article-**h**ole excited-states we obtain at the same time the theoretical energy and theoretical spin →→→ A. Bohr hypothesis:

$$\boxed{I \approx M^*}$$

$$E^* = \sum_p e_{p,m_p} - \sum_h e_{h,m_h} \quad \text{and} \quad I \approx M^* = \sum_p m_p - \sum_h m_h$$

Tilted Fermi Surface: Energy Minimisation at Fixed Spin

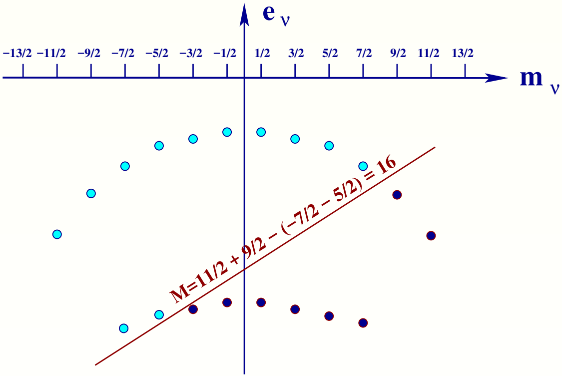

For the **p**article-**h**ole excited-states we obtain at the same time the theoretical energy and theoretical spin $\rightarrow\rightarrow\rightarrow$ A. Bohr hypothesis:

$$\boxed{I \approx M^*}$$

$$E^* = \sum_p e_{p,m_p} - \sum_h e_{h,m_h} \quad \text{and} \quad I \approx M^* = \sum_p m_p - \sum_h m_h$$

Some Particle-Hole Excitations Generate Yrast-Traps

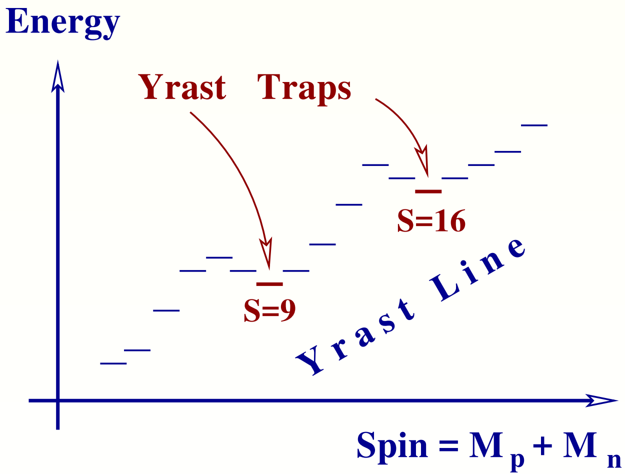

$$E^* = \sum_p e_{p,m_p} - \sum_h e_{h,m_h} \quad \text{and} \quad I \approx M^* = \sum_p m_p - \sum_h m_h$$

K-Isomers

Example: ^{147}Gd – Realistic Calculations

K-Isomers

Example: ^{147}Gd – Realistic Calculations

Realistic Phenomenological Mean Field
Universal Parametrisation: (Z,N)-Plane

A Powerful Tool: Tilted Fermi Surface Method (I)

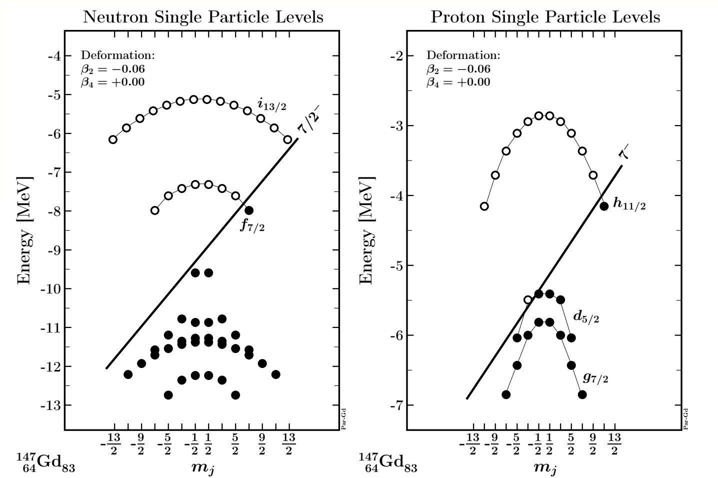

- Theoretically suggested spin $I = \frac{7}{2} + 7 = \frac{21}{2}$ $\rightarrow$ Prediction: $I^\pi = \frac{21}{2}^+$

A Powerful Tool: Tilted Fermi Surface Method (I)

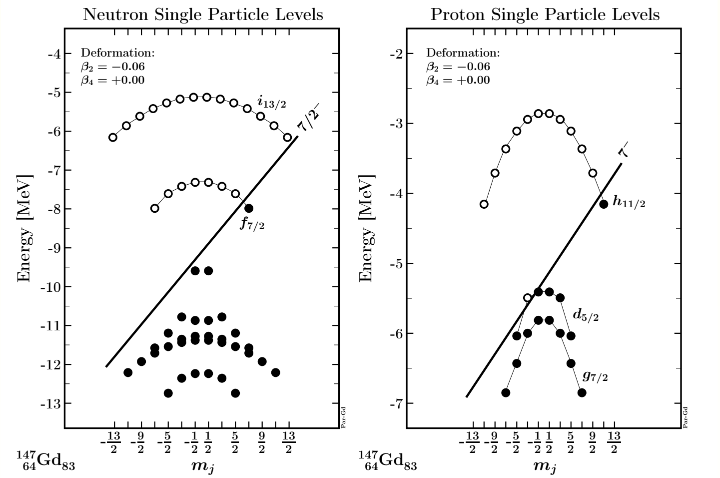

Experiment : $I^{\pi}_{exp.} = \frac{21}{2}^{+}$ **(4.55 ns)** $\leftrightarrow$ Mean Field theory $I^{\pi}_{mf} = \frac{21}{2}^{+}$

A Powerful Tool: Tilted Fermi Surfaces - (II)

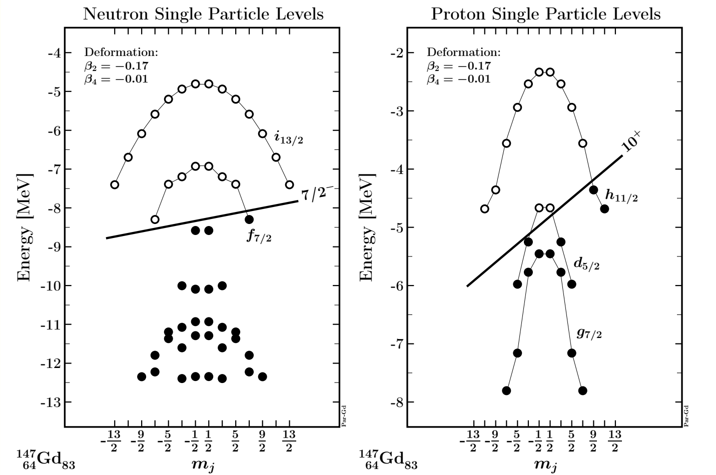

- Theoretically suggested spin $I = \frac{7}{2} + 10 = \frac{27}{2}$ $\rightarrow$ Prediction: $I^\pi = \frac{27}{2}^-$

A Powerful Tool: Tilted Fermi Surfaces - (II)

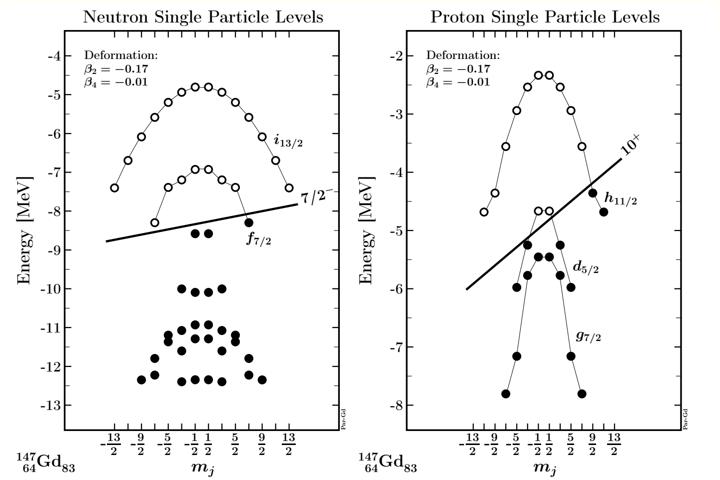

Experiment : $I^{\pi}_{exp.} = \frac{27}{2}^{-}$ **(26.8 ns)** $\leftrightarrow$ Mean Field theory $I^{\pi}_{mf} = \frac{27}{2}^{-}$

A Powerful Tool: Tilted Fermi Surfaces - (III)

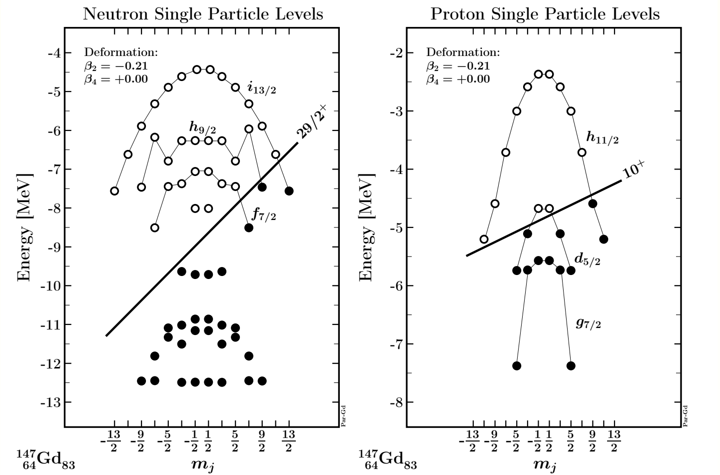

- Theoretically suggested spin $I = \frac{29}{2} + 10 = \frac{49}{2} \rightarrow$ Prediction: $I^{\pi} = \frac{49}{2}^{+}$

A Powerful Tool: Tilted Fermi Surfaces - (III)

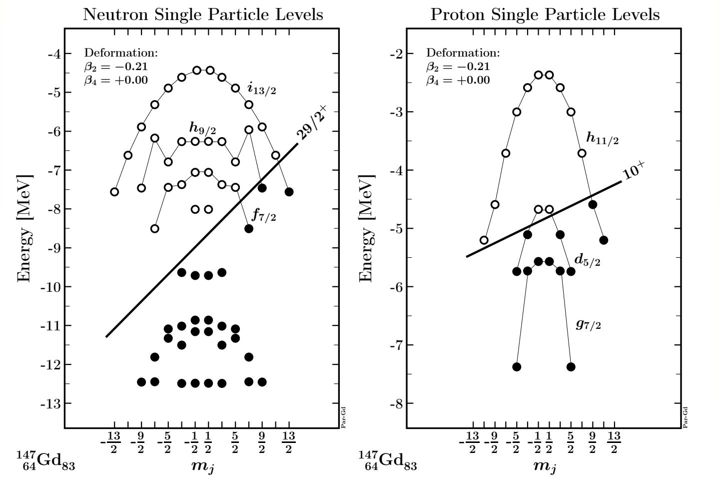

Experiment : $I^{\pi}_{exp.} = \frac{49}{2}^{+}$ **(510 ns)** $\leftrightarrow$ Mean Tield theory $I^{\pi}_{mf} = \frac{49}{2}^{+}$

These isomers were known for over 30 years or so...

What About the "Newer" Isomers in ^{147}Gd?

Negative Parity Isomers in ^{147}Gd - (IV)

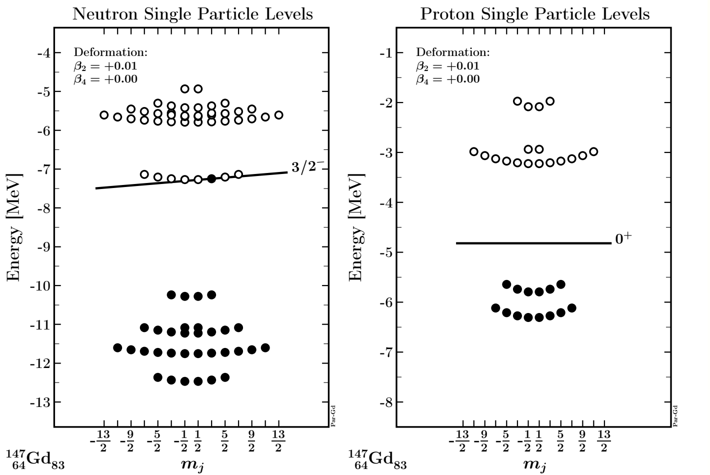

- Theoretically suggested spin $I = \frac{3}{2} + 0 = \frac{3}{2} \rightarrow$ Prediction: $I^\pi = \frac{3}{2}^-$

Negative Parity Isomers in ^{147}Gd - (IV)

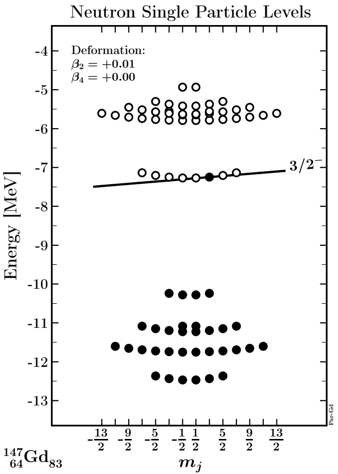

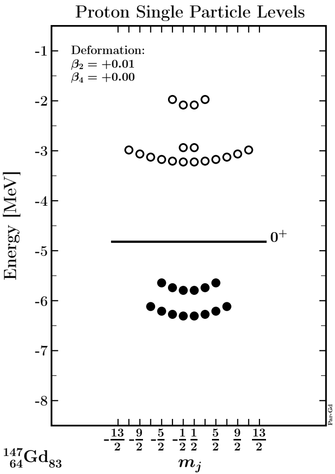

Experiment : $I^{\pi}_{exp.} = \frac{3}{2}^{-}$ **(0.2 ns)** $\leftrightarrow$ Mean Field theory $I^{\pi}_{mf} = \frac{3}{2}^{-}$

Negative Parity Isomers in ^{147}Gd - (V)

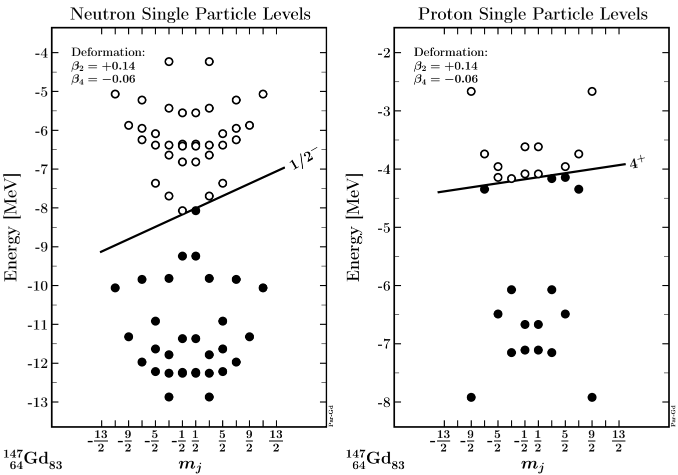

- Theoretically suggested spin $I = \frac{1}{2} + 4 = \frac{9}{2} \rightarrow$ Prediction: $I^\pi = \frac{9}{2}^-$

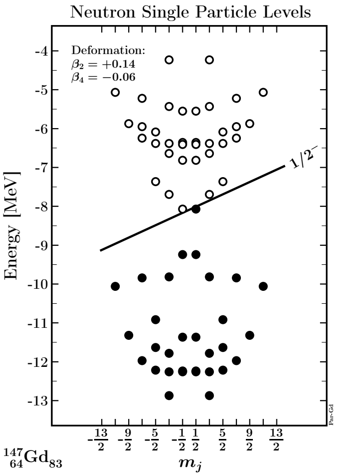

Experiment : $\mathrm{I}^{\pi}_{\mathrm{exp.}} = \frac{9}{2}^{-}$ **(0.35 ns)** $\leftrightarrow$ Mean Field theory $\mathrm{I}^{\pi}_{\mathrm{mf}} = \frac{9}{2}^{-}$

Negative Parity Isomers in ^{147}Gd - (VI)

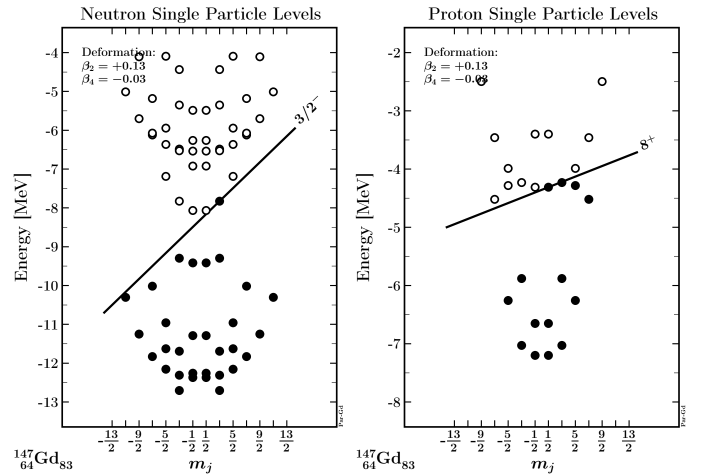

- Theoretically suggested spin $I = \frac{3}{2} + 8 = \frac{19}{2}$ → Prediction: $I^\pi = \frac{19}{2}^-$

Negative Parity Isomers in ^{147}Gd - (VI)

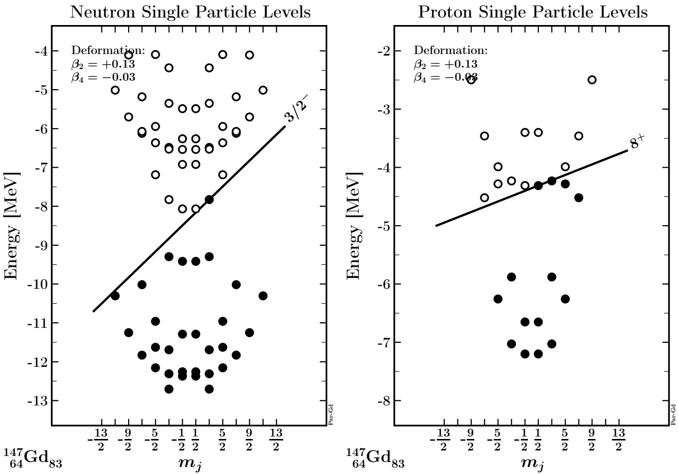

$$\text{Experiment : } I^{\pi}_{\text{exp.}} = \frac{19}{2}^{-} \textbf{(0.37 ns)} \;\leftrightarrow\; \text{Mean Field theory } I^{\pi}_{\text{mf}} = \frac{19}{2}^{-}$$

Positive Parity Isomers in ^{147}Gd - (VII)

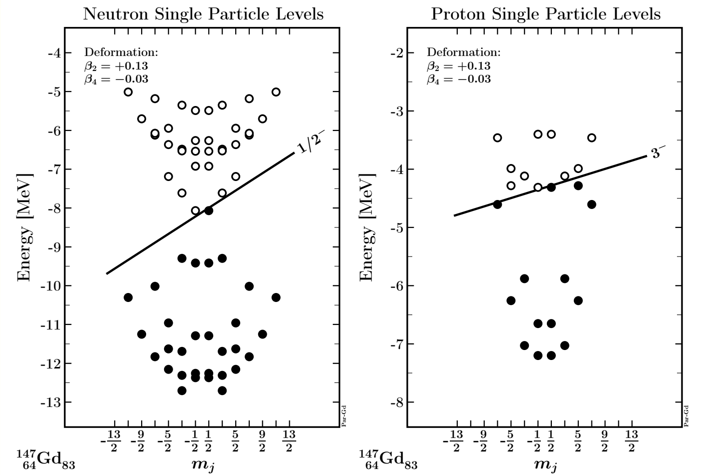

- Theoretically suggested spin $I = \frac{1}{2} + 3 = \frac{7}{2} \rightarrow$ Prediction: $I^\pi = \frac{7}{2}^+$

Positive Parity Isomers in ^{147}Gd - (VII)

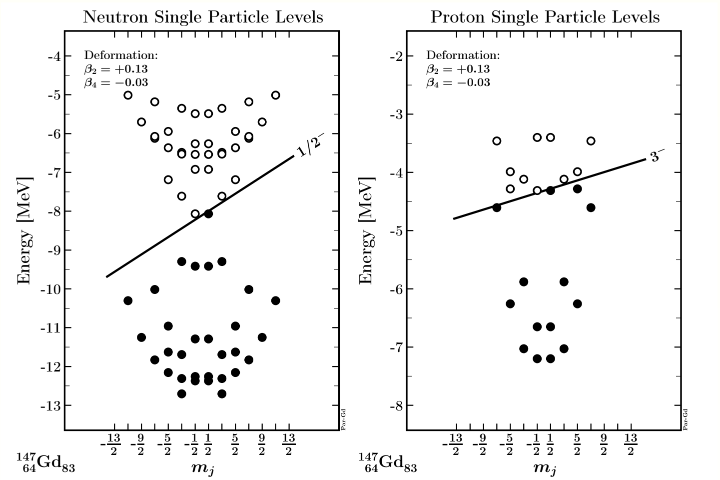

$$\text{Experiment}: \mathrm{I}^{\pi}_{\text{exp.}} = \frac{7}{2}^{+}(\mathbf{0.42\,ns}) \;\leftrightarrow\; \text{Mean Field theory } \mathrm{I}^{\pi}_{\text{mf}} = \frac{7}{2}^{+}$$

Positive Parity Isomers in ^{147}Gd - (VIII)

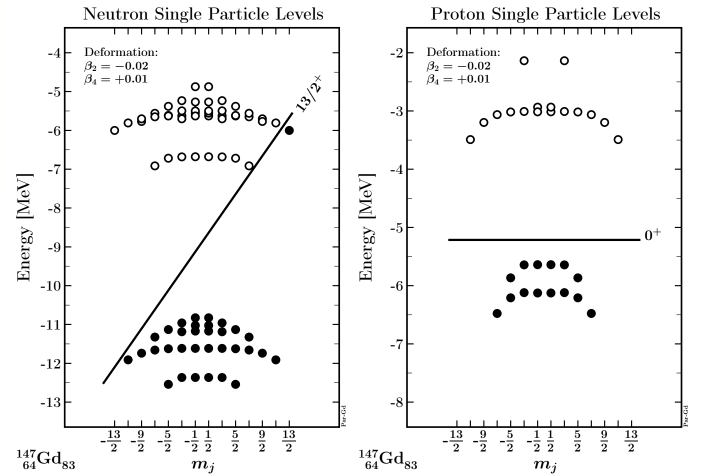

- Theoretically suggested spin $I = \frac{13}{2} + 0 = \frac{13}{2}$ $\rightarrow$ Prediction: $I^\pi = \frac{13}{2}^+$

Positive Parity Isomers in ^{147}Gd - (VIII)

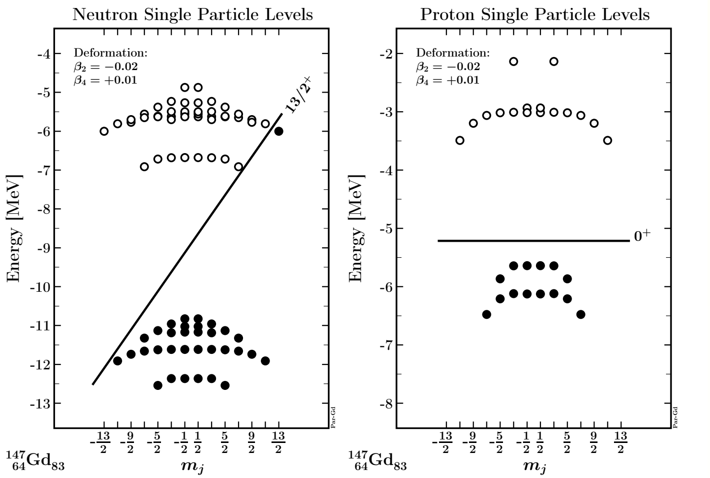

$$\text{Experiment} : I^{\pi}_{\text{exp.}} = \frac{13}{2}^{+} (\mathbf{21.4\,ns}) \leftrightarrow \text{Mean} - \text{Field theory } I^{\pi}_{\text{mf}} = \frac{13}{2}^{+}$$

Theory ↔ Full Experimental Confirmation

- **Summary**: All 8 double titled Fermi surface solutions for ^{147}Gd (lowest energy solutions according to Bohr tilted Fermi hypothesis) **correspond to the experimentally confirmed results**

No.	I^π	I_p^π	I_n^π	Isomer Lifetime
1	$3/2^-$	0^+	$3/2^-$	0.20 ns
2	$7/2^+$	3^-	$1/2^-$	0.42 ns
3	$9/2^-$	4^+	$1/2^-$	0.35 ns
4	$13/2^+$	0^+	$13/2^+$	21.4 ns
5	$19/2^-$	8^+	$3/2^-$	0.37 ns
6	$21/2^+$	7^-	$7/2^-$	4.55 ns
7	$27/2^-$	10^+	$7/2^-$	26.8 ns
8	$49/2^+$	10^+	$29/2^+$	510 ns
	...	...	...	...

Another Illustration of the Axial Symmetry and K-Conservation

Calculating Nuclear Yrast Lines

• **Yrast line: Attention! Highly non-trivial numerical effort involving $N \sim 10^6$ particle-hole configurations! Minimised over α_{20}, α_{40}, etc.**

• **Yrast line: Attention! Highly non-trivial numerical effort involving $N \sim 10^6$ particle-hole configurations! Minimised over α_{20}, α_{40}, etc.**

• Here: Yrast ^{147}Gd sequence calculated using the realistic phenomenological WS-universal mean field approach.

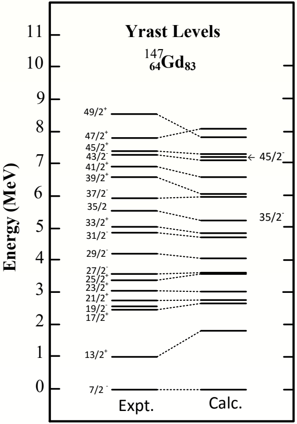

- **Yrast line: Attention! Highly non-trivial numerical effort involving** **$N \sim 10^6$ particle-hole configurations! Minimised over α_{20}, α_{40}, etc.**

- Here: Yrast ^{147}Gd sequence calculated using the realistic phenomenological WS-universal mean field approach.

- The energy of each state has been minimised over several axial-symmetry deformation parameters.

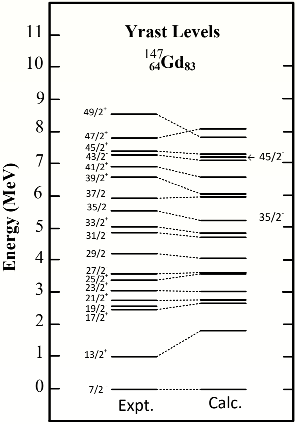

• **Yrast line: Attention! Highly non-trivial numerical effort involving** **$N \sim 10^6$ particle-hole configurations! Minimised over α_{20}, α_{40}, etc.**

• Here: Yrast ^{147}Gd sequence calculated using the realistic phenomenological WS-universal mean field approach.

• The energy of each state has been minimised over several axial-symmetry deformation parameters.

• We consider the number of mean-field configurations comparable to the sizes of the typical spherical shell-model Hamiltonian.

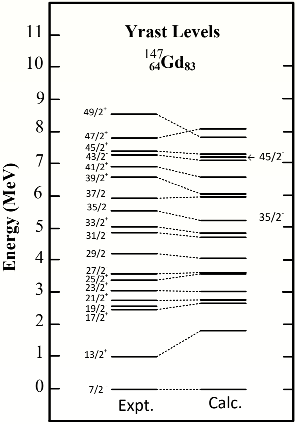

• **Yrast line: Attention! Highly non-trivial numerical effort involving $\underline{\underline{N \sim 10^6}}$ particle-hole configurations! Minimised over α_{20}, α_{40}, etc.**

• Here: Yrast ^{147}Gd sequence calculated using the realistic phenomenological WS-universal mean field approach.

• The energy of each state has been minimised over several axial-symmetry deformation parameters.

• We consider the number of mean-field configurations comparable to the sizes of the typical spherical shell-model Hamiltonian.

• It is natural to ask:

How many parameters have been fitted to obtain the result on the right?

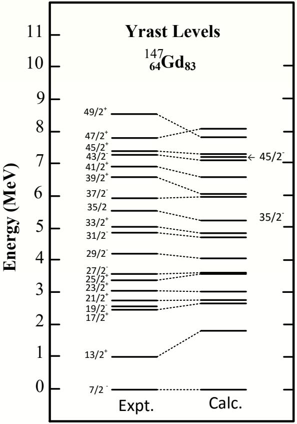

One can also say:

The quality of the description is a sign of "predictive power"

One can also say:

The quality of the description is a sign of “predictive power”

- Is this i n s t e a d just the case of *reproduction by fitting?*

One can also say:

The quality of the description is a sign of "predictive power"

- Is this i n s t e a d just the case of *reproduction by fitting?*
  - Or rather a manifestation of *predictive power?*

One can also say:

The quality of the description is a sign of "predictive power"

- Is this i n s t e a d just the case of *reproduction by fitting?*
  - Or rather a manifestation of *predictive power?*

In other words: How many parameters are fitted to spectra?

One can also say:

The quality of the description is a sign of "predictive power"

- Is this i n s t e a d just the case of *reproduction by fitting?*
    - Or rather a manifestation of *predictive power?*

In other words: How many parameters are fitted to spectra?

NONE – no parameter adjusted to the presented data;
This is what is meant as Woods-Saxon Universal mean-field

What Do We Learn
From Measuring K-Isomers?

What Do We Learn From Measuring K-Isomers?

• **K-isomers may live longer or even much longer compared with the related ground states $\rightarrow$ This allows extending the experimental accessibility to the New Areas of Exotic Nuclei!**

What Do We Learn From Measuring K-Isomers?

• K-isomers may live longer or even much longer compared with the related ground states $\rightarrow$ This allows extending the experimental accessibility to the New Areas of Exotic Nuclei!

• The life-times of K-isomers vary dramatically over many orders of magnitude providing the precious information about:

– The configuration changes via decay: (np-nh) $\rightarrow$ (n'p-n'h)

– Signals of spontaneous axial-symmetry breaking [K-mixing]

What Do We Learn From Measuring K-Isomers?

What Do We Learn From Measuring K-Isomers?

• **Establish areas of existence of axial symmetry, as opposed to non-axiality, throughout the Periodic Table. But: Why some (Z,N)-combinations induce axial symmetry and others do not?**

What Do We Learn From Measuring K-Isomers?

• **Establish areas of existence of axial symmetry, as opposed to non-axiality, throughout the Periodic Table. But: Why some (Z,N)-combinations induce axial symmetry and others do not?**

• **The axial-symmetry nuclei may choose to rotate collectively**

$$\boxed{(\vec{I} \perp \mathcal{O}_{\text{symmetry}}) \; - \; \textbf{bands}}$$

as alternative to

$$\boxed{(\vec{I} \parallel \mathcal{O}_{\text{symmetry}}) \; - \; \textbf{isomers}}$$

or both at the same shape at the same time (in competition).

Why? Which mechanisms cause this or that behaviour?

Section 3

Collective Rotation, Band Crossings and Back-bending

The well known Hartree-Fock-Bogolyubov Cranking (HFBC) Method

Potential energy surfaces provide the full choice of competing minima

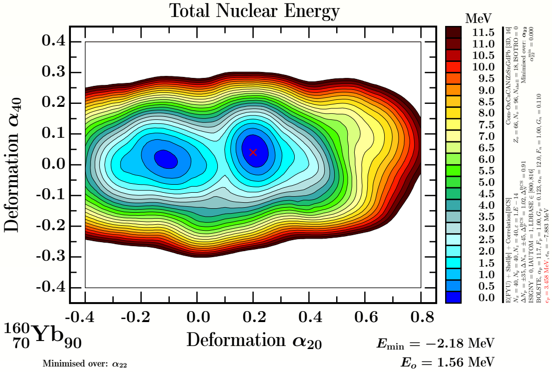

• Knowing the equilibrium deformation we may employ the Hartree-Fock-Bogolyubov Cranking (HFBC) user code $\rightarrow$ Find the moments of inertia

Hartree Fock Bogolyubov Cranking ↔ Back-Bending

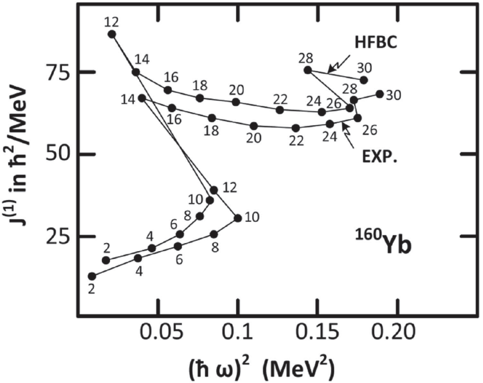

- Universal W-S mean field offers excellent comparison with experiment

The user will have access to a contemporary plotting code

Hartree Fock Bogolyubov Cranking ↔ Back-Bending

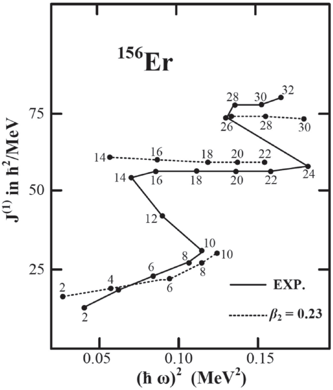

- Universal W-S mean field offers excellent comparison with experiment
  The user will have access to a contemporary plotting code

Section 4

Tracing Shape Transitions and Corresponding Probabilities in $\mathcal{N}$-Dimensional Deformation Spaces

How to treat realistically the nuclear motion in multidimensional spaces?

Proposed Solution: Apply Graph Theory and multi-dimensional Dijkstra Algorithm

The Issue: We Completed a 4D Mesh Run... And?

- **With $\sim$2 000 000 deformation points $\leftrightarrow$ nuclear potential energies**
- **We wish to discuss results in order to propose some experiments**

The Issue: We Completed a 4D Mesh Run... And?

- **With ∼2 000 000 deformation points ↔ nuclear potential energies**
- **We wish to discuss results in order to propose some experiments**
- **Example from literature ↔ we wish to produce something similar**

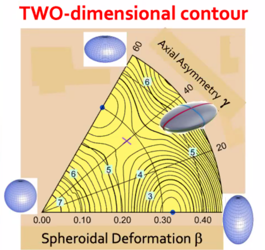

Stolen from Silvia – Sorry!

The Issue: We Completed a 4D Mesh Run... And?

- **With $\sim$2 000 000 deformation points $\leftrightarrow$ nuclear potential energies**
- **We wish to discuss results in order to propose some experiments**
- **Example from literature $\leftrightarrow$ we wish to produce something similar**

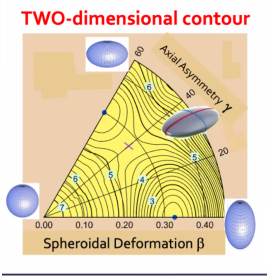

Stolen from Silvia – Sorry!

- **How to do it?**

The Issue: We Completed a 4D Mesh Run... And?

- **With $\sim$2 000 000 deformation points $\leftrightarrow$ nuclear potential energies**
- **We wish to discuss results in order to propose some experiments**
- **Example from literature $\leftrightarrow$ we wish to produce something similar**

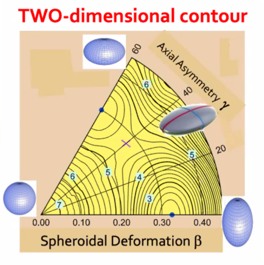

Stolen from Silvia – Sorry!

- **How to do it? We have six 2D projections possible in 4D space: Should we take one? Which one? Does it make sense? Not at all!**

- We wish to calculate 4D transition probabilities between preselected 2 minima
- Map composition: $\mathcal{N}_1 \cdot \mathcal{N}_2 \sim 3 \times 10^3$ points; Space of $\mathcal{N}_1 \cdot \mathcal{N}_2 \cdot \mathcal{N}_3 \cdot \mathcal{N}_4 \sim 2.5 \times 10^6$

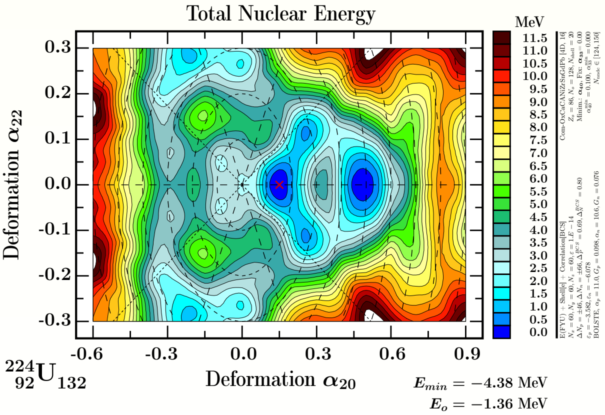

- How to connect correctly 2 points among 2.5×10^6 knowing only 3×10^3 ???

*) $\mathcal{N}_1 = 61, \ \mathcal{N}_2 = 49, \ \mathcal{N}_3 = 33, \ \mathcal{N}_4 = 25$

The following illustrations have a heuristic character

("pedagogical purposes")

• In its simplest formulation, Dijkstra algorithm provides a distance between points, say Q_1 and Q_2, in an n-dimensional space of variables $\{q^i\}$:

$$\boxed{d \equiv \int_{Q_1}^{Q_2} ds, \quad \text{where} \quad ds \equiv \left\{\sum_{i=1}^{n} M^{ij} dq_i dq_i\right\}^{1/2}}$$

• We introduce a number, say $\mathcal{N}$, of discrete points referred to as *vertices*

• The pairs of those points are considered connected by paths called *edges*

• Each edge has attributed one positive number $\rightarrow$ called *length* or *weight*

• Any sequence of a number of connected nodes is referred to as a *graph*

• Any graph with only one path between every two nodes is called a *tree*

Graph Theory (Dijkstra Algorithm) within One Page

• In its simplest formulation, Dijkstra algorithm provides a distance between points, say Q_1 and Q_2, in an n-dimensional space of variables $\{q^i\}$:

$$\boxed{d \equiv \int_{Q_1}^{Q_2} ds, \quad \text{where} \quad ds \equiv \left\{\sum_{i=1}^{n} M^{ij}\, dq_i\, dq_i\right\}^{1/2}}$$

• We introduce a number, say $\mathcal{N}$, of discrete points referred to as *vertices*

• The pairs of those points are considered connected by paths called *edges*

• Each edge has attributed one positive number $\rightarrow$ called *length* or *weight*

• Any sequence of a number of connected nodes is referred to as a *graph*

• Any graph with only one path between every two nodes is called a *tree*

Dijkstra algorithm solves the basic problem of finding the path of minimal total length between two given vertices of interest

Graph Theory (Dijkstra Algorithm) within One Page

• In its simplest formulation, Dijkstra algorithm provides a distance between points, say Q_1 and Q_2, in an n-dimensional space of variables $\{q^i\}$:

$$\boxed{d \equiv \int_{Q_1}^{Q_2} ds, \quad \text{where} \quad ds \equiv \left\{\sum_{i=1}^{n} M^{ij}\, dq_i\, dq_i\right\}^{1/2}}$$

• We introduce a number, say $\mathcal{N}$, of discrete points referred to as *vertices*

• The pairs of those points are considered connected by paths called *edges*

• Each edge has attributed one positive number $\rightarrow$ called *length* or *weight*

• Any sequence of a number of connected nodes is referred to as a *graph*

• Any graph with only one path between every two nodes is called a *tree*

Suppose you are the boss of the transport company in charge of furnishing goods to 10 CORA magazines over motorways and normal roads from 50 storage places; You download the Dijkstra code and determine most economical transportation mode

Dijkstra Algorithm $\leftrightarrow$ Nuclear Octupole Mesh

- The set of $\mathcal{N}$ nodes consists of 4 deformation coordinates: α_{30}, α_{31}, α_{32}, α_{33}
- We have a 4D hyper-cube $\alpha_{3,\mu} \in [-0.30, +0.30]$, interdistances $\Delta\alpha_{3,\mu} = 0.025$
- There are 25 points along each axis $\rightarrow$ total number of vertices $\mathcal{N}_\mathrm{v} = 390625$
- It follows that graph has $\mathcal{N}_\mathrm{e} = 152587500000 \sim 1.5 \times 10^{11}$ connecting edges
- For the sake of the present applications, we use the WKB probability formula

$$\boxed{P(E) = \exp\left\{-2\int_{Q_1}^{Q_2} \sqrt{\frac{2\mu}{\hbar^2}\Big[V[q(s)] - E\Big]}\, ds\right\}},$$

discretised in such a way that every pair of vertices is replaced by Q_1 and Q_2:

$$\Delta P_{1\rightarrow 2} = \int_{Q_1}^{Q_2} \sqrt{\bar{V} - E}\, ds \;\; \text{where} \;\; \bar{V} \overset{df.}{=} \frac{1}{2}\left[V(Q_1) + V(Q_2)\right]$$

- The edges of the graph, say $\mathcal{G}$, have attributed their weights, which are the 'distances' between the nodes in the sense of the semi-classical WKB probability

Dijkstra Algorithm: Example of Application

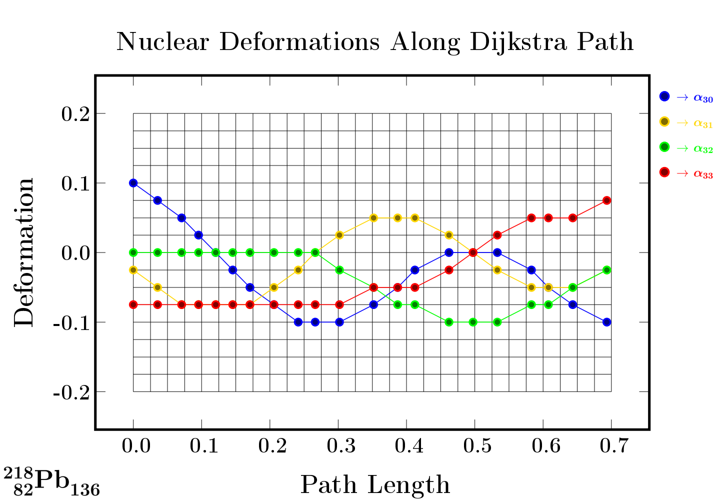

- Example of solution connecting 2 points in 4D space; The program provides the potential height along the motion path and transition probability (life time)

Synthetic Conclusions

- **We can solve the problem of connecting any two points in an N-dimensional deformation space in a mathematically correct manner using graph theory of Applied Mathematics**

- **A small price to pay: We use the WKB approximation, otherwise common in nuclear structure physics**

- **Among applications on the list: Fission life-times along competing paths**

Section 5

New Suggestions for Spectroscopy

Example: 4-Fold Octupole Magic Number N = 136

- Mean-field $\hat{Q}_{\lambda=3}$ repulsion between $2g_{9/2}$ and $1j_{15/2}$ neutron orbitals

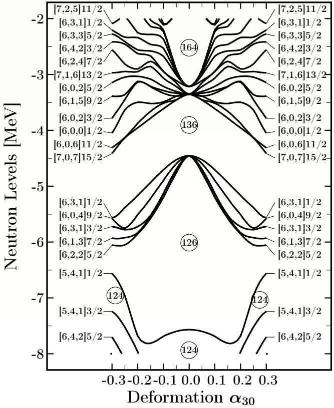

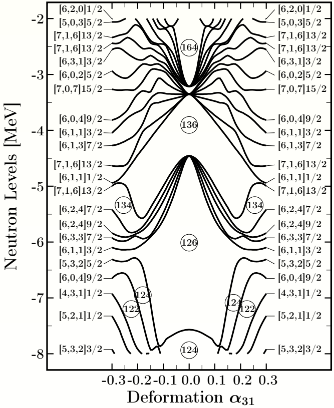

- **Notice octupole $N = 136$ shell gap above spherical $N = 126$ shell gap**

- Mean-field $\hat{Q}_{\lambda=3}$ repulsion between $2g_{9/2}$ and $1j_{15/2}$ neutron orbitals

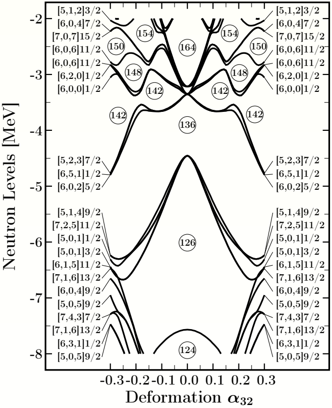

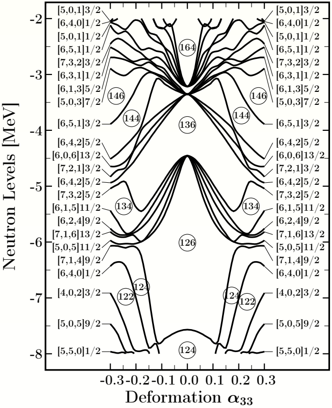

- **Notice octupole $N = 136$ shell gap above spherical $N = 126$ shell gap**

To emphasise: Tetrahedral symmetry gap α_{32} almost as large as $N = 126$

- **Thanks to the octupole 4-fold magic number $N = 136$ multipoles $\lambda = 3$ (octupole) rather than $\lambda = 2$ introduce non-sphericity $\rightarrow$ exotic deformations & symmetries**

The 4-fold Octupole Magic Number N=136

• Thanks to the octupole 4-fold magic number $N = 136$
multipoles $\lambda = 3$ (octupole) rather than $\lambda = 2$
introduce non-sphericity $\rightarrow$ exotic deformations & symmetries

• What are the corresponding implications for the ground-state minima?

Pb Looses Sphericity for increasing N – Because of $\alpha_{3\mu}$ and NOT $\alpha_{2\mu}$

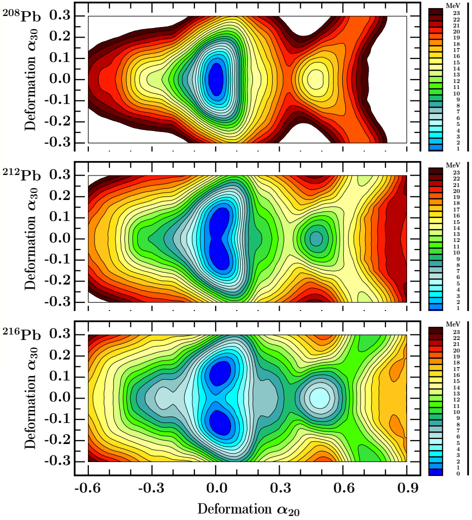

- **Pb nuclei loose sphericity at $\alpha_{20} = 0$: NO "PROLATE-OBLATE" slang**

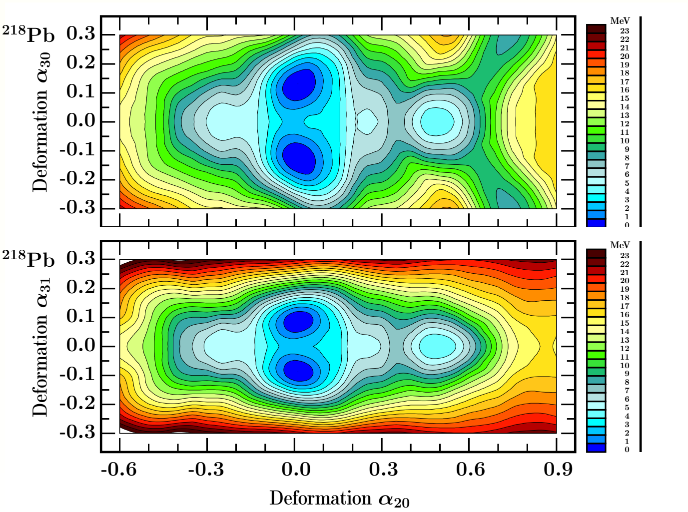

- **Note the predicted octupole (not quadrupole) non-sphericity: $^{218}\mathrm{Pb}_{136}$**

- Large barriers, over 3 MeV, separating double tetrahedral minima

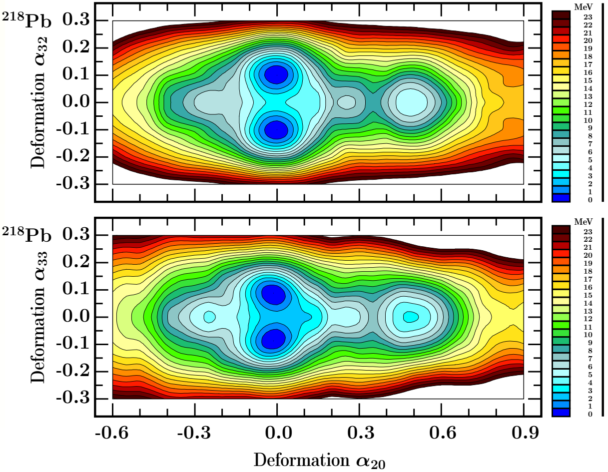

- **Note the predicted octupole (not quadrupole) non-sphericity: $^{218}\mathrm{Pb}_{136}$**

Good for Exotic Symmetries!!

- **We define Exotic Symmetries as anything but ellipsoidal $(\alpha_{20}, \alpha_{22})$ or pear-shape $(\alpha_{20}, \alpha_{30})$**

Good for Exotic Symmetries!!

- **We define Exotic Symmetries as anything but ellipsoidal $(\alpha_{20}, \alpha_{22})$ or pear-shape $(\alpha_{20}, \alpha_{30})$**

- **Thanks to the octupole 4-fold $N = 136$ magic number multipoles $\lambda = 3$ (octupole) rather than $\alpha_{\lambda=2}$ (quadrupole) win introducing non-sphericity & exotic symmetries**

• **We define Exotic Symmetries as anything but ellipsoidal (α_{20}, α_{22}) or pear-shape (α_{20}, α_{30})**

• **Thanks to the octupole 4-fold $N = 136$ magic number multipoles $\lambda = 3$ (octupole) rather than $\alpha_{\lambda=2}$ (quadrupole) win introducing non-sphericity & exotic symmetries**

What are these exotic molecular symmetries?

- **Symmetry induced by both $\alpha_{31} \neq 0$ and $(\alpha_{20} \neq 0, \alpha_{31} \neq 0)$**

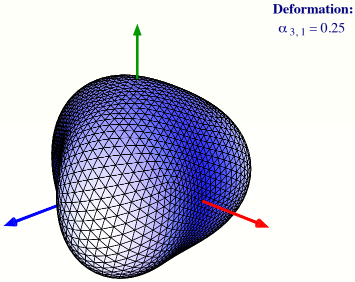

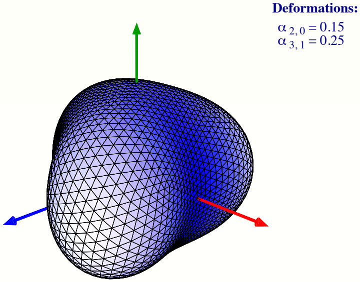

$\boldsymbol{\alpha_{31} = 0.25}$

$\boldsymbol{\alpha_{20} = 0.15, \alpha_{31} = 0.25}$

Nuclear C_{2v} Point Group Symmetry

- **Symmetry induced by both $\alpha_{33} \neq 0$ and $(\alpha_{20} \neq 0, \alpha_{33} \neq 0)$**

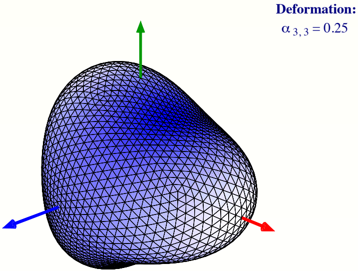

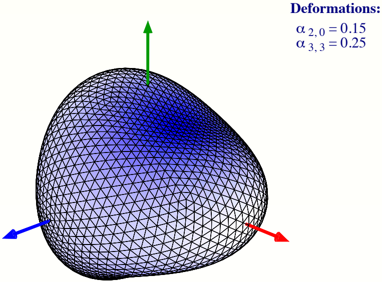

$\alpha_{33} = 0.25$ $\alpha_{20} = 0.15, \alpha_{33} = 0.25$

Nuclear D_{3h} Point Group Symmetry

- **Symmetry induced by $\alpha_{32} \neq 0$ and $(\alpha_{20} \neq 0, \alpha_{32} \neq 0)$**

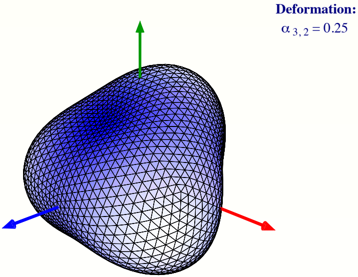

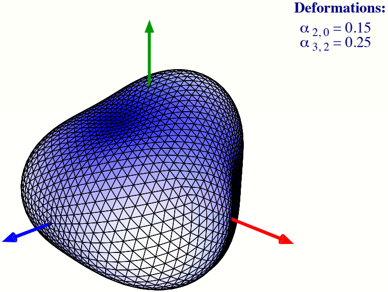

Tetrahedral T_d: $\alpha_{32} = 0.25$

D_{2d}: $\alpha_{20} = 0.15, \alpha_{32} = 0.25$

$$\boxed{\textbf{Nuclear } T_d \textbf{ and } D_{2d} \textbf{ Point Group Symmetries}}$$

And now:

Let us address what we call

New Spectroscopy: Issues & Challenges

Theory Predicted Properties: T_d vs. O_h Bands

- The tetrahedral symmetry group has 5 irreducible representations
- The ground-state $I^\pi = 0^+$ belongs to A_1 representation given by:

$$\underbrace{\mathrm{A}_1: \quad 0^+, 3^-, 4^+, \underbrace{(6^+, 6^-)}_{\text{doublet}}, 7^-, 8^+, \underbrace{(9^+, 9^-)}_{\text{doublet}}, \underbrace{(10^+, 10^-)}_{\text{doublet}}, 11^-, \underbrace{2 \times 12^+, 12^-}_{\text{triplet}}, \cdots}_{\textbf{Forming a common parabola}}$$

- There are no states with spins $I = 1, 2$ and 5. We have parity doublets: $I = 6, 9, 10 \ldots$, at energies: $E_{6^-} = E_{6^+}$, $E_{9^-} = E_{9^+}$, etc.

Theory Predicted Properties: $\mathrm{T_d}$ vs. $\mathrm{O_h}$ Bands

- The tetrahedral symmetry group has 5 irreducible representations
- The ground-state $I^\pi = 0^+$ belongs to A_1 representation given by:

$$\underbrace{\mathrm{A}_1: \quad 0^+,\, 3^-,\, 4^+,\, \underbrace{(6^+, 6^-)}_{\text{doublet}},\, 7^-,\, 8^+,\, \underbrace{(9^+, 9^-)}_{\text{doublet}},\, \underbrace{(10^+, 10^-)}_{\text{doublet}},\, 11^-,\, \underbrace{2\times 12^+,\, 12^-}_{\text{triplet}},\, \cdots}_{\textbf{Forming a common parabola}}$$

- There are no states with spins $I = 1, 2$ and 5. We have parity doublets: $I = 6, 9, 10 \ldots$, at energies: $E_{6^-} = E_{6^+}$, $E_{9^-} = E_{9^+}$, etc.

- One shows that the analogue structure in the octahedral symmetry

$$\underbrace{A_{1g}:\ 0^+, 4^+, 6^+, 8^+, 9^+, 10^+,\ \ldots,\ \ I^\pi = I^+}_{\textbf{Forming a common parabola}}$$

$$\underbrace{A_{2u}:\ 3^-, 6^-, 7^-, 9^-, 10^-, 11^-, \ldots,\ I^\pi = I^-}_{\textbf{Forming another (common) parabola}}$$

Theory Predicted Properties: $\mathrm{T_d}$ vs. $\mathrm{O_h}$ Bands

- The tetrahedral symmetry group has 5 irreducible representations
- The ground-state $I^\pi = 0^+$ belongs to A_1 representation given by:

$$\underbrace{\mathrm{A}_1: \quad 0^+,\, 3^-,\, 4^+,\, \underbrace{(6^+, 6^-)}_{\text{doublet}},\, 7^-,\, 8^+,\, \underbrace{(9^+, 9^-)}_{\text{doublet}},\, \underbrace{(10^+, 10^-)}_{\text{doublet}},\, 11^-,\, \underbrace{2\times 12^+,\, 12^-}_{\text{triplet}},\, \cdots}_{\textbf{Forming a common parabola}}$$

- There are no states with spins $I = 1, 2$ and 5. We have parity doublets: $I = 6, 9, 10 \ldots$, at energies: $E_{6^-} = E_{6^+}$, $E_{9^-} = E_{9^+}$, etc.
- One shows that the analogue structure in the octahedral symmetry

$$\underbrace{A_{1g}: \; 0^+, 4^+, 6^+, 8^+, 9^+, 10^+, \; \ldots, \;\; I^\pi = I^+}_{\textbf{Forming a common parabola}}$$

$$\underbrace{A_{2u}: \; 3^-, 6^-, 7^-, 9^-, 10^-, 11^-, \ldots, \;\; I^\pi = I^-}_{\textbf{Forming another (common) parabola}}$$

Consequently we should expect two independent parabolic structures

Theory Confirmed by Experiment up to Details

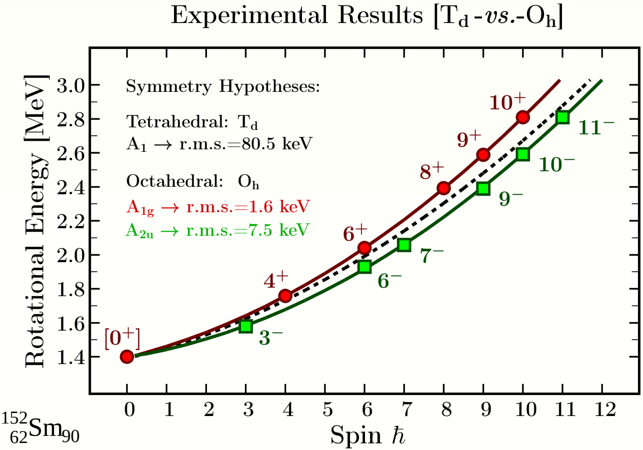

Graphical representation of the experimental data from the summary Table. Curves represent the fit and are *not* meant 'to guide the eye'. Markedly, point $[I^\pi = 0^+]$, is a prediction by extrapolation - not an experimental datum.

The first tetrahedral symmetry evidence based on the experimental data

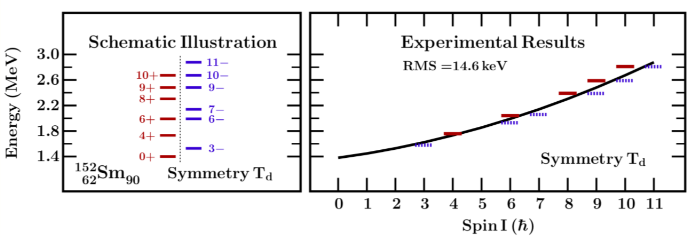

Tetrahedral Band : $I^{\pi}_{T_d} = 0^+, 3^-, 4^+, 6^\pm, 7^-, 8^+, 9^\pm, 10^\pm, 11^-, \ldots$

→ **Published in: J. Dudek et al., PHYSICAL REVIEW C 97, 021302(R) (2018)**

The first tetrahedral symmetry evidence based on the experimental data

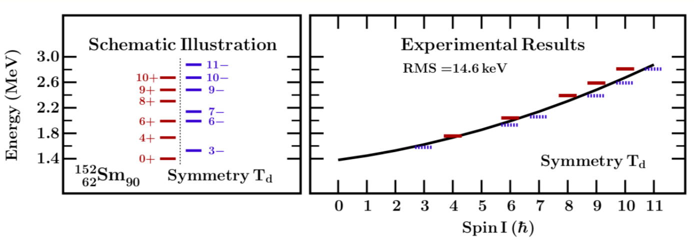

Tetrahedral Band : $I^{\pi}_{T_d} = 0^+, 3^-, 4^+, 6^{\pm}, 7^-, 8^+, 9^{\pm}, 10^{\pm}, 11^-, \ldots$

→ **Published in: J. Dudek et al., PHYSICAL REVIEW C 97, 021302(R) (2018)**

- **Analysing NNDC experimental evidence for ^{152}Sm took 3 months of manual work**

We can apply the same group-theory methods which we used to determine the $\mathrm{T_d}$ & $\mathrm{O_h}$ band structures

Illustrations follow $\rightarrow$

- Rotational band structure of a nucleus in a C_{2v}-symmetric configuration

$$
\begin{aligned}
C_{2v} \rightarrow A_1: \quad & 0^+, \\
& 1^-, \\
& 2\times 2^+,\ 2^-, \\
& 3^+,\ 2\times 3^-, \\
& 3\times 4^+,\ 2\times 4^-, \\
& 2\times 5^+,\ 3\times 5^-, \\
& 4\times 6^+,\ 3\times 6^-, \\
& 3\times 7^+,\ 4\times 7^-, \\
& 5\times 8^+,\ 4\times 8^-, \\
& 4\times 9^+,\ 5\times 9^-, \\
& 6\times 10^+,\ 5\times 10^-, \\
& 5\times 11^+,\ 6\times 11^-, \\
& 7\times 12^+,\ 6\times 12^-,\ \ldots
\end{aligned}
$$

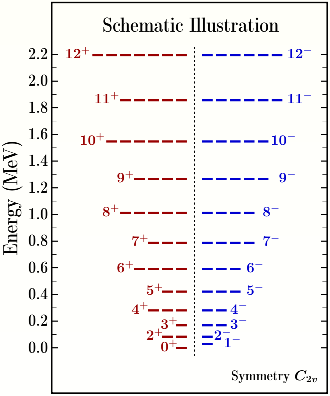

Degeneracy pattern $(\alpha_{20}, \alpha_{31})$

These methods are powerful:

See the world first experimental evidence

of the nuclear C_{2v} symmetry in ^{236}U

- Rotational band structure of a nucleus in a C_{2v}-symmetric configuration

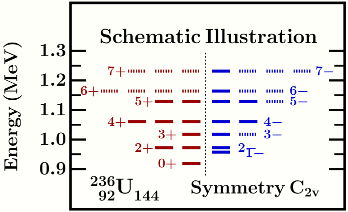

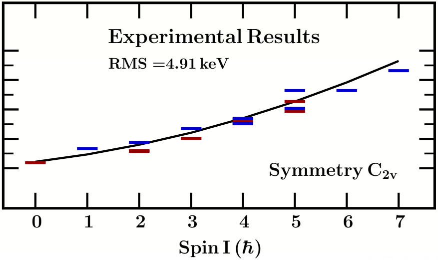

Conclusions of Application-Illustration Part

- **Download the slides and analyse the content focussing on: Computer codes already installed or "under installation" ?**
- **In most of the cases you are offered alternative NEW (no-standard or simply unknown solutions)**
- **Typical example (prolate/oblate shape coexistences) known over 2 centuries, NOW replaced by numerous frontier research alternatives**

Section 6

Imagining Nucleons in a Nucleus

Section 6

Imagining Nucleons in a Nucleus

Spatial Structure of Orbitals

Section 6

Imagining Nucleons in a Nucleus

Spatial Structure of Orbitals

In other words: Let's see where nucleons are?

Spatial Structure of Orbitals (Sperical ^{132}Sn) ($|\psi(\vec{r})|^2$)

Limit 80%

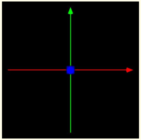

Limit ??%

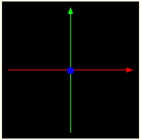

Limit ??%

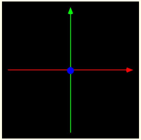

Limit ??%

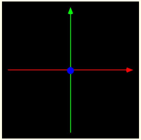

Limit ??%

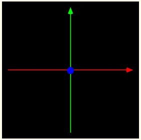

Density distribution $|\psi_\pi(\vec{r})|^2 \geq$ Limit, for $\pi = [2,0,2]1/2$ orbital

Spatial Structure of Orbitals (Sperical ^{132}Sn) ($|\psi(\vec{r})|^2$)

Limit 80%

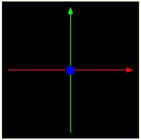

Limit 50%

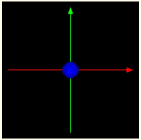

Limit ??%

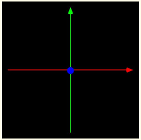

Limit ??%

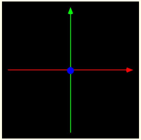

Limit ??%

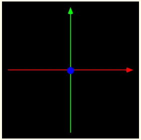

Density distribution $|\psi_\pi(\vec{r})|^2 \geq$ Limit, for $\pi = [2,0,2]1/2$ orbital

Spatial Structure of Orbitals (Sperical ^{132}Sn) ($|\psi(\vec{r})|^2$)

Limit 80%

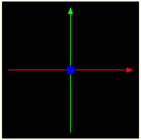

Limit 50%

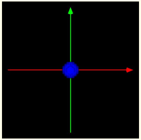

Limit 10%

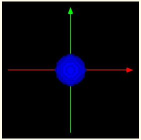

Limit ??%

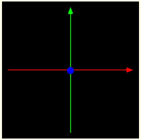

Limit ??%

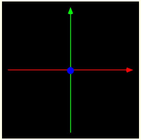

Density distribution $|\psi_\pi(\vec{r})|^2 \geq$ Limit, for $\pi = [2, 0, 2]1/2$ orbital

Spatial Structure of Orbitals (Sperical ^{132}Sn) ($|\psi(\vec{r})|^2$)

Limit 80%

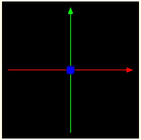

Limit 50%

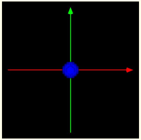

Limit 10%

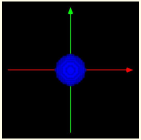

Limit 3%

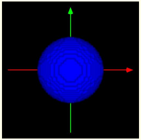

Limit ??%

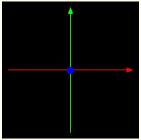

Density distribution $|\psi_\pi(\vec{r})|^2 \geq$ Limit, for $\pi = [2, 0, 2]1/2$ orbital

Spatial Structure of Orbitals (Sperical ^{132}Sn) ($|\psi(\vec{r})|^2$)

Limit 80%

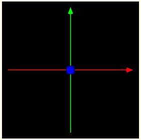

Limit 50%

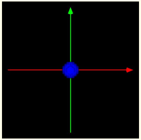

Limit 10%

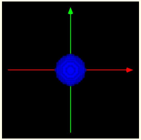

Limit 3%

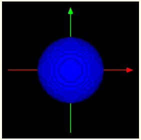

Limit 1%

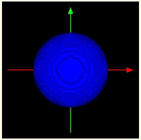

Density distribution $|\psi_\pi(\vec{r})|^2 \geq$ Limit, for $\pi = [2,0,2]1/2$ orbital

Spatial Structure of Orbitals (Sperical ^{132}Sn) ($|\psi(\vec{r})|^2$)

Limit 80%

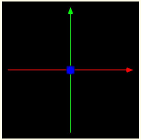

Limit 50%

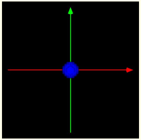

Limit 10%

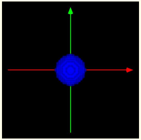

Limit 3%

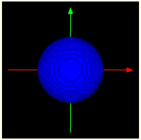

Limit 1%

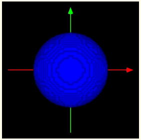

Limit 20%

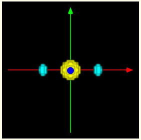

Limit ??%

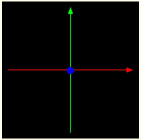

Limit ??%

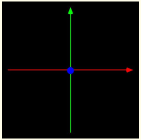

Limit ??%

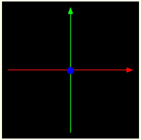

Limit ??%

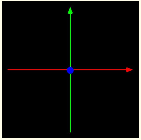

Bottom: N=3 shell b-[303]7/2, w-[312]5/2, y-[321]3/2, p-[310]1/2

Spatial Structure of Orbitals (Sperical ^{132}Sn) ($|\psi(\vec{r})|^2$)

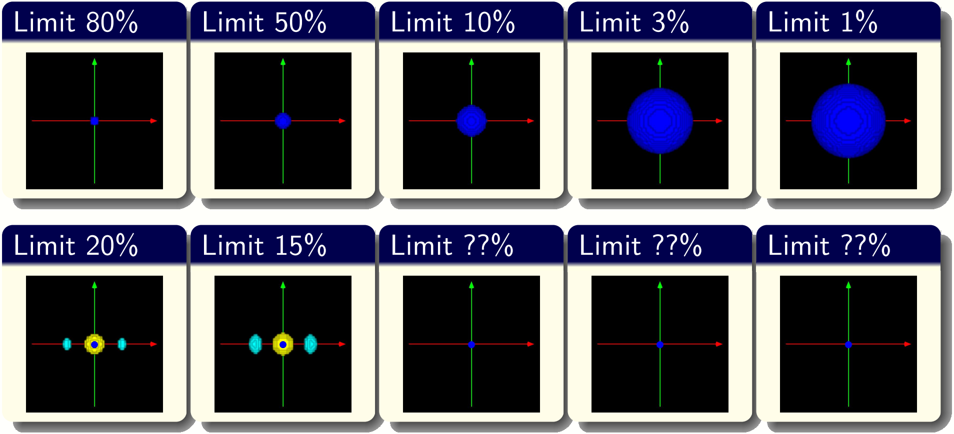

Bottom: N=3 shell b-[303]7/2, w-[312]5/2, y-[321]3/2, p-[310]1/2

Spatial Structure of Orbitals (Sperical ^{132}Sn) ($|\psi(\vec{r})|^2$)

Limit 80%

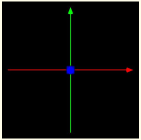

Limit 50%

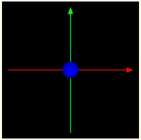

Limit 10%

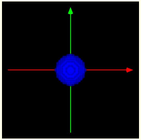

Limit 3%

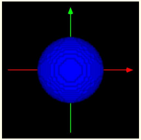

Limit 1%

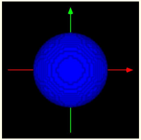

Limit 20%

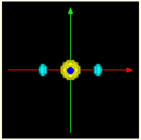

Limit 15%

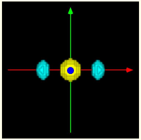

Limit 12%

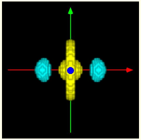

Limit ??%

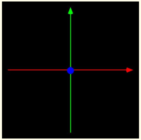

Limit ??%

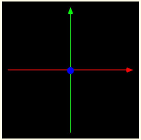

Bottom: N=3 shell b-[303]7/2, w-[312]5/2, y-[321]3/2, p-[310]1/2

Spatial Structure of Orbitals (Sperical ^{132}Sn) ($|\psi(\vec{r})|^2$)

Limit 80%

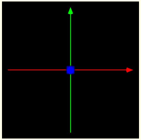

Limit 50%

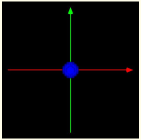

Limit 10%

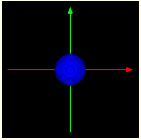

Limit 3%

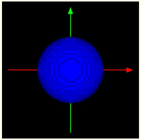

Limit 1%

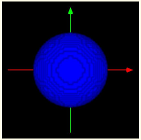

Limit 20%

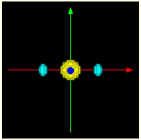

Limit 15%

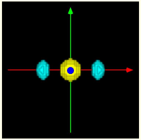

Limit 12%

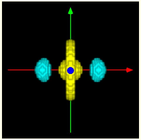

Limit 10%

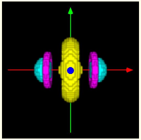

Limit ??%

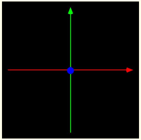

Bottom: N=3 shell b-[303]7/2, w-[312]5/2, y-[321]3/2, p-[310]1/2

Spatial Structure of Orbitals (Sperical ^{132}Sn) ($|\psi(\vec{r})|^2$)

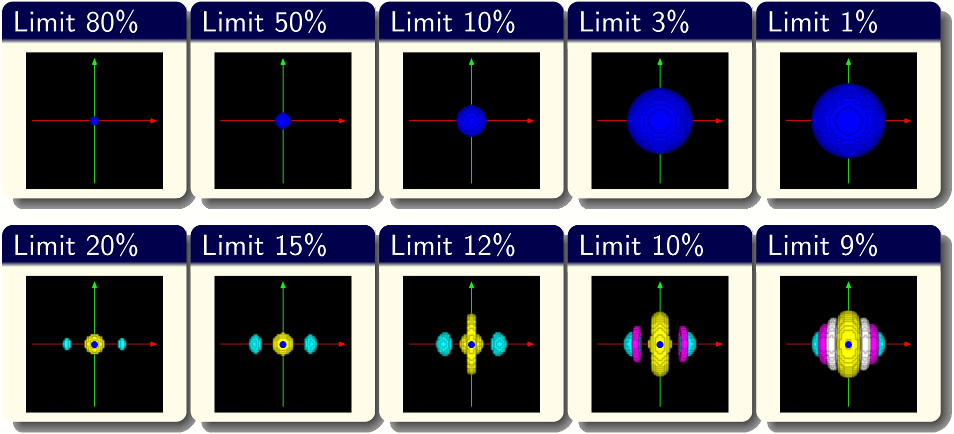

Bottom: N=3 shell b-[303]7/2, w-[312]5/2, y-[321]3/2, p-[310]1/2

Spatial Structure of N=3 Spherical Shell ($|\psi_\nu(\vec{r})|^2$)

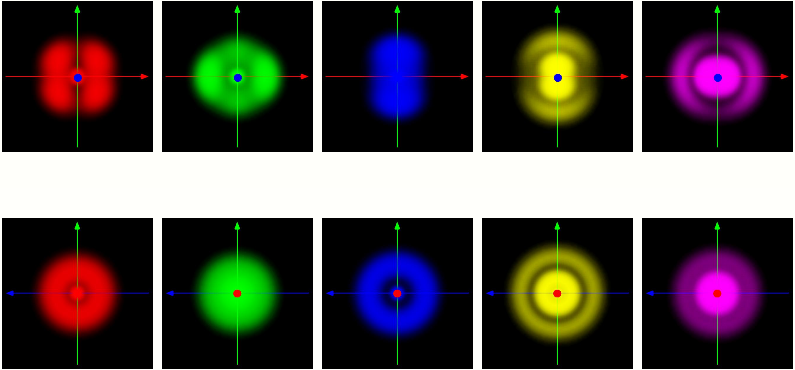

^{132}Sn: Distributions $|\psi_\nu(\vec{r})|^2$ for single proton orbitals. Top $\mathcal{O}_{xz}$, bottom $\mathcal{O}_{yz}$. Proton $e_\nu \leftrightarrow [\nu{=}30, 32, \ldots 38]$ for spherical shell

Spatial Structure of N=3 Spherical Shell ($|\psi_\nu(\vec{r})|^2$)

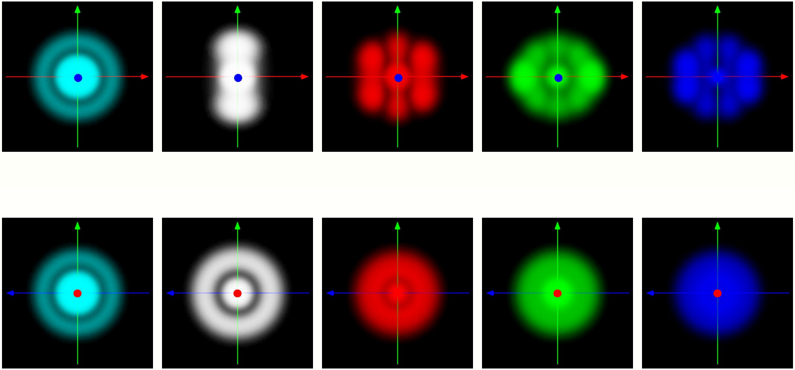

^{132}Sn: Distributions $|\psi_\nu(\vec{r})|^2$ for single proton orbitals. Top $\mathcal{O}_{xz}$, bottom $\mathcal{O}_{yz}$. Proton $e_\nu \leftrightarrow [\nu{=}40, 42, \ldots 48]$ for spherical shell

Spatial Structure of N=3 Spherical Shell ($|\psi_\nu(\vec{r})|^2$)

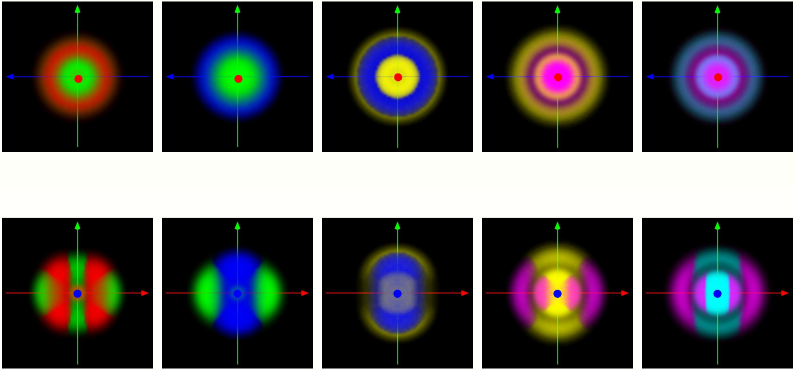

^{132}Sn: distributions $|\psi_\nu(\vec{r})|^2$ for consecutive pairs of orbitals. Top $\mathcal{O}_{xz}$, bottom $\mathcal{O}_{yz}$. Proton $e_\nu \leftrightarrow$ [n=30:32, ... 38:40], spherical shell

Spatial Structure of N=3 Spherical Shell ($|\psi_\nu(\vec{r})|^2$)

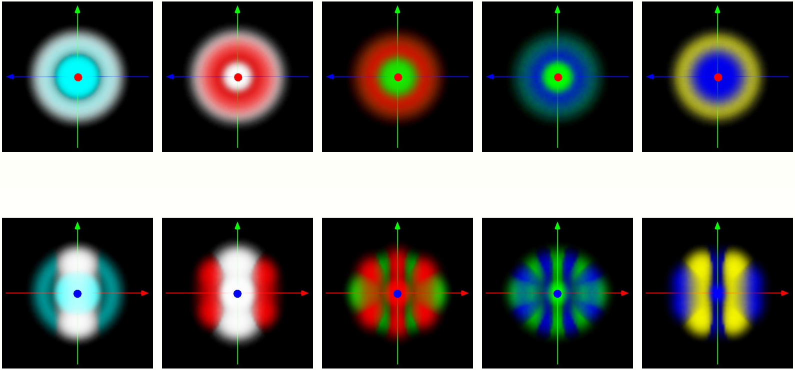

^{132}Sn: distributions $|\psi_\nu(\vec{r})|^2$ for consecutive pairs of orbitals. Top $\mathcal{O}_{xz}$, bottom $\mathcal{O}_{yz}$. Proton $e_\nu \leftrightarrow [n{=}40{:}42, \ldots\ 48{:}50]$, spherical shell

The First Octahedral Shell (20 Nucleons)) ($|\psi(\vec{r})|^2$)

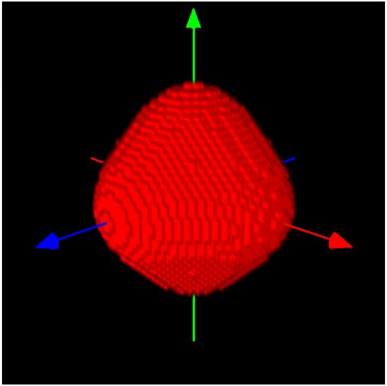

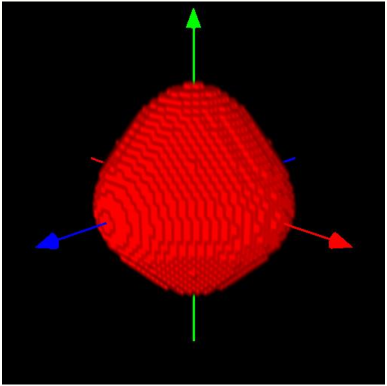

Left: accumulating image of all orbitals; Right: Single Orbital (No.1)

The First Octahedral Shell (20 Nucleons)) ($|\psi(\vec{r})|^2$)

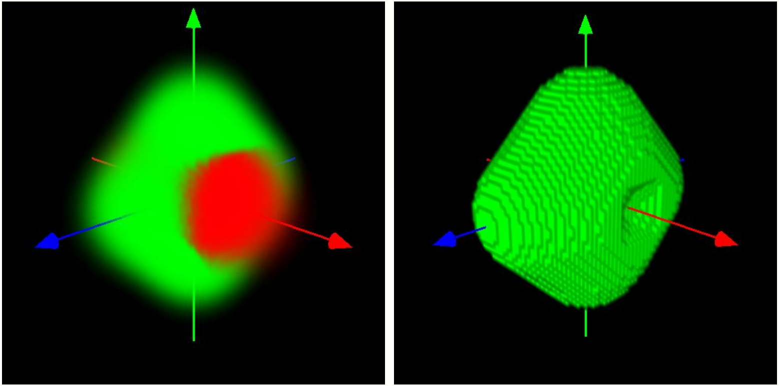

Left: accumulating image of all orbitals; Right: Single Orbital (No.2)

The First Octahedral Shell (20 Nucleons)) ($|\psi(\vec{r})|^2$)

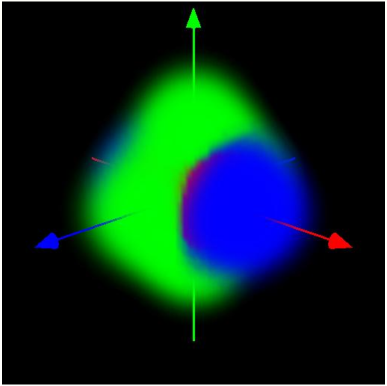

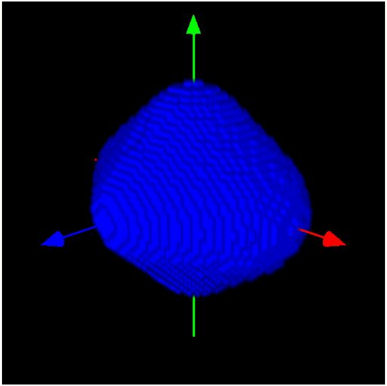

Left: accumulating image of all orbitals; Right: Single Orbital (No.3)

The First Octahedral Shell (20 Nucleons)) ($|\psi(\vec{r})|^2$)

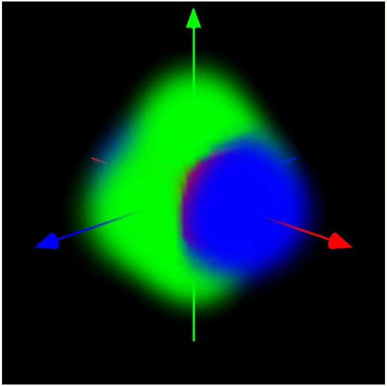

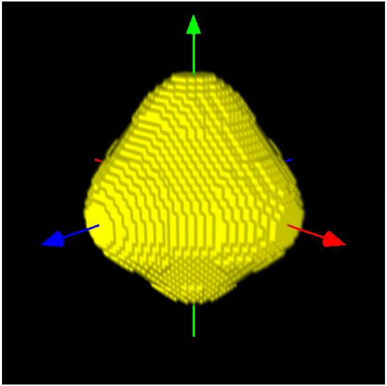

Left: accumulating image of all orbitals; Right: Single Orbital (No.4)

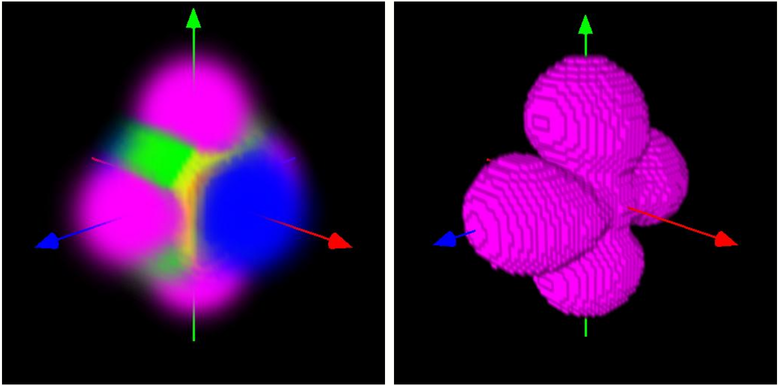

Left: accumulating image of all orbitals; Right: Single Orbital (No.5)

The First Octahedral Shell (20 Nucleons)) ($|\psi(\vec{r})|^2$)

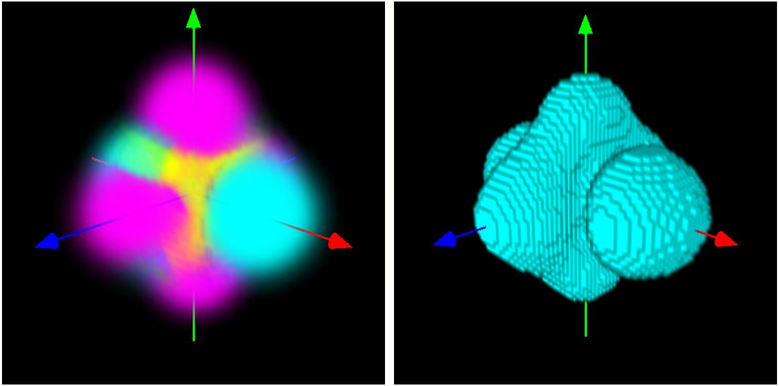

Left: accumulating image of all orbitals; Right: Single Orbital (No.6)

The First Octahedral Shell (20 Nucleons)) ($|\psi(\vec{r})|^2$)

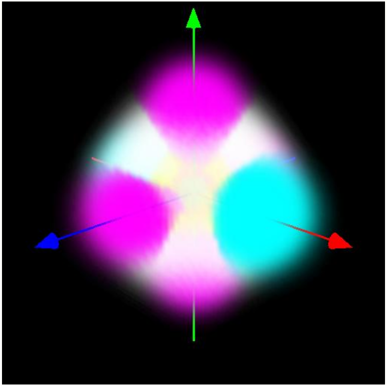

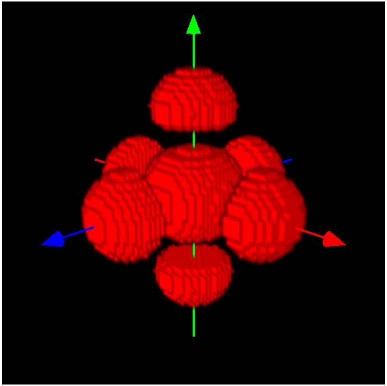

Left: accumulating image of all orbitals; Right: Single Orbital (No.7)

The First Octahedral Shell (20 Nucleons)) ($|\psi(\vec{r})|^2$)

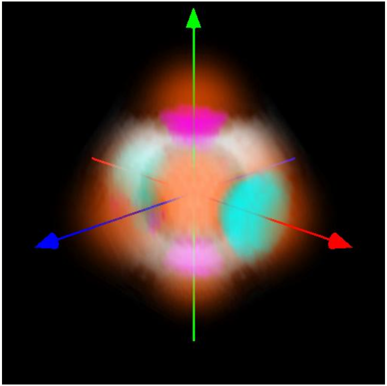

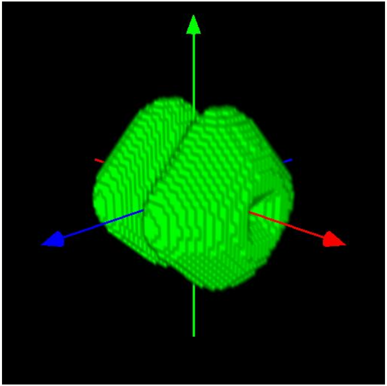

Left: accumulating image of all orbitals; Right: Single Orbital (No.8)

The First Octahedral Shell (20 Nucleons)) ($|\psi(\vec{r})|^2$)

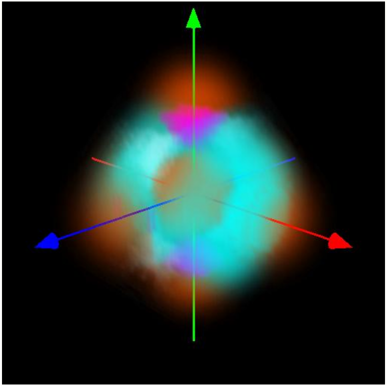 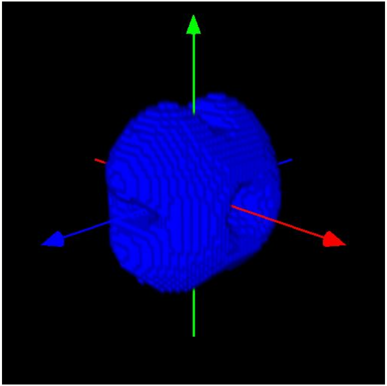

Left: accumulating image of all orbitals; Right: Single Orbital (No.9)

The First Octahedral Shell (20 Nucleons)) ($|\psi(\vec{r})|^2$)

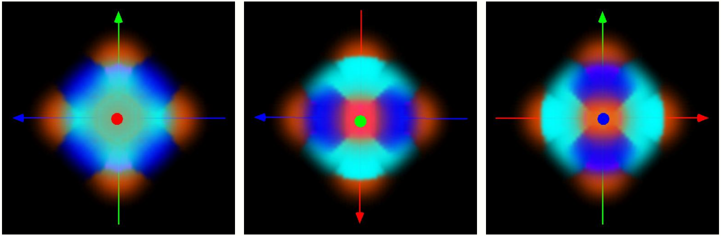

Three space perspectives of the full octahedral shell (n=20 nucleons)

Back to Euro-Labs Internet Site

Back to Euro-Labs Internet Site

Reviewing the Options

Back to Euro-Labs Internet Site

Reviewing the Options

A compact View

Wave-Function Spatial Analysis in ^{208}Pb, N=64 Onwards

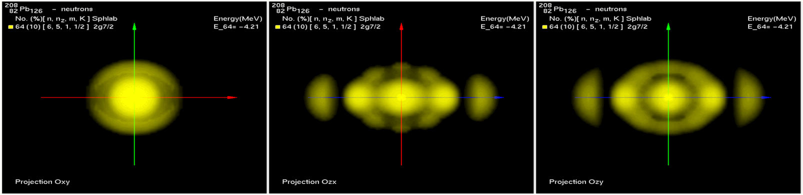

Wave-Function Spatial Analysis in ^{208}Pb, N=64 Onwards

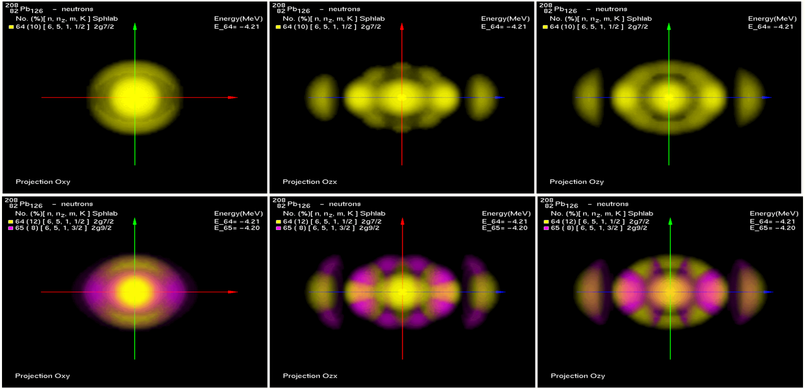

Wave-Function Spatial Analysis in ^{208}Pb, N=64 Onwards

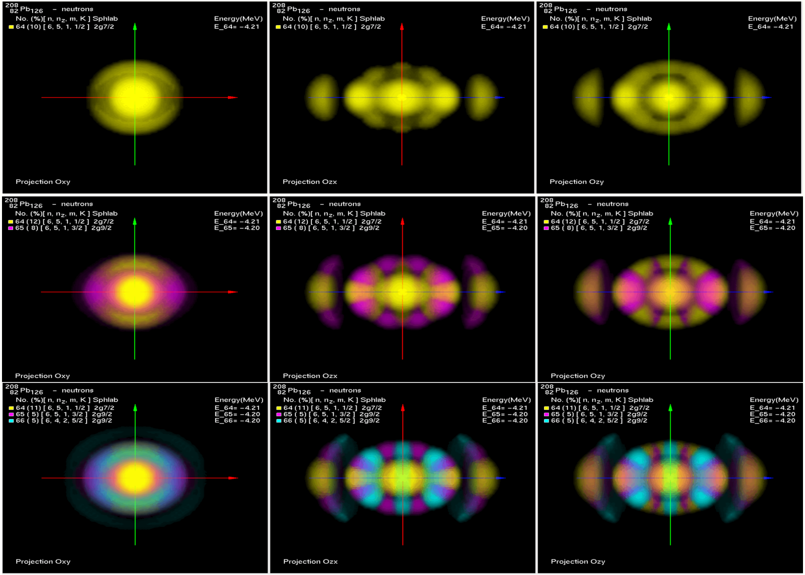

Wave-Function Spatial Analysis in ^{208}Pb, N=67 Onwards

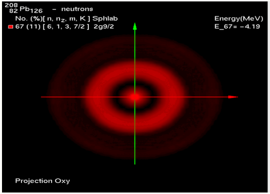

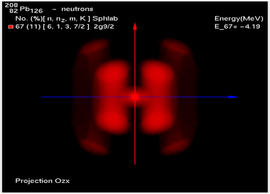

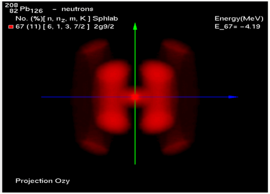

Wave-Function Spatial Analysis in ^{208}Pb, N=67 Onwards

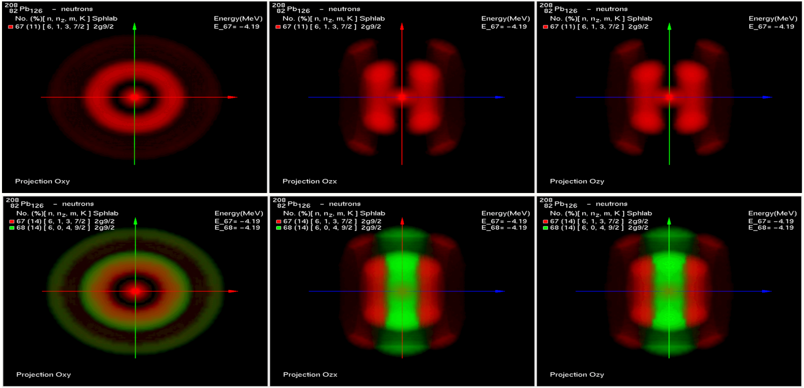

Wave-Function Spatial Analysis in ^{208}Pb, N=67 Onwards

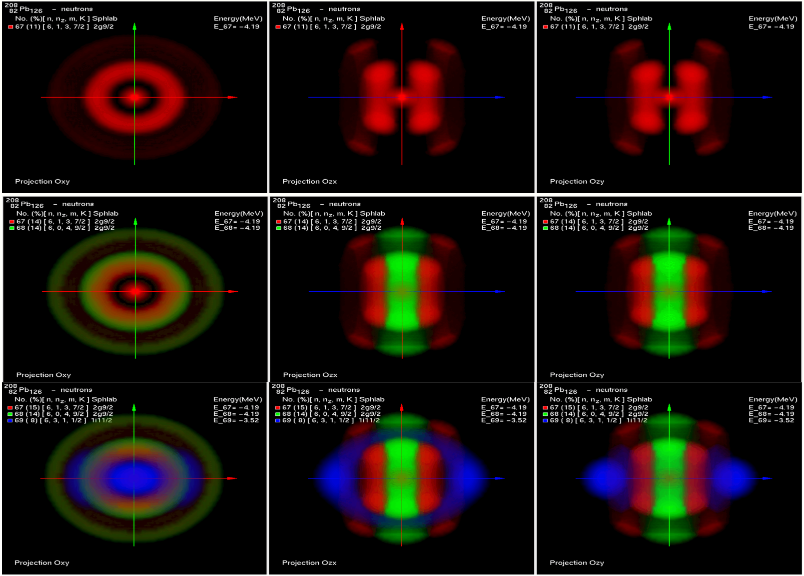

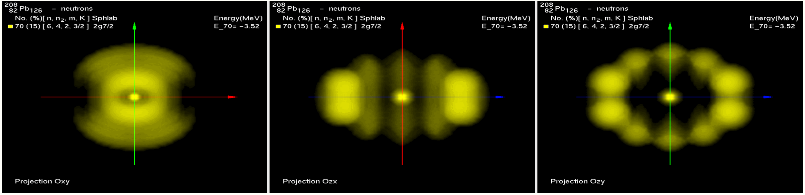
$^{208}_{82}Pb_{126}$ – neutrons
No. (%)[n, n_z, m, K] Sphlab
70 (15) [6, 4, 2, 3/2] 2g7/2
Energy(MeV)
E_70= −3.52
Projection Oxy
$^{208}_{82}Pb_{126}$ – neutrons
No. (%)[n, n_z, m, K] Sphlab
70 (15) [6, 4, 2, 3/2] 2g7/2
Energy(MeV)
E_70= −3.52
Projection Ozx
$^{208}_{82}Pb_{126}$ – neutrons
No. (%)[n, n_z, m, K] Sphlab
70 (15) [6, 4, 2, 3/2] 2g7/2
Energy(MeV)
E_70= −3.52
Projection Ozy

Wave-Function Spatial Analysis in ^{208}Pb, N=70 Onwards

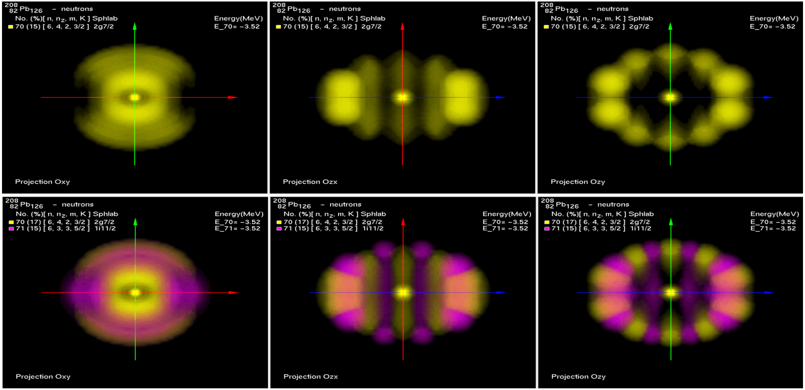

Wave-Function Spatial Analysis in ^{208}Pb, N=70 Onwards

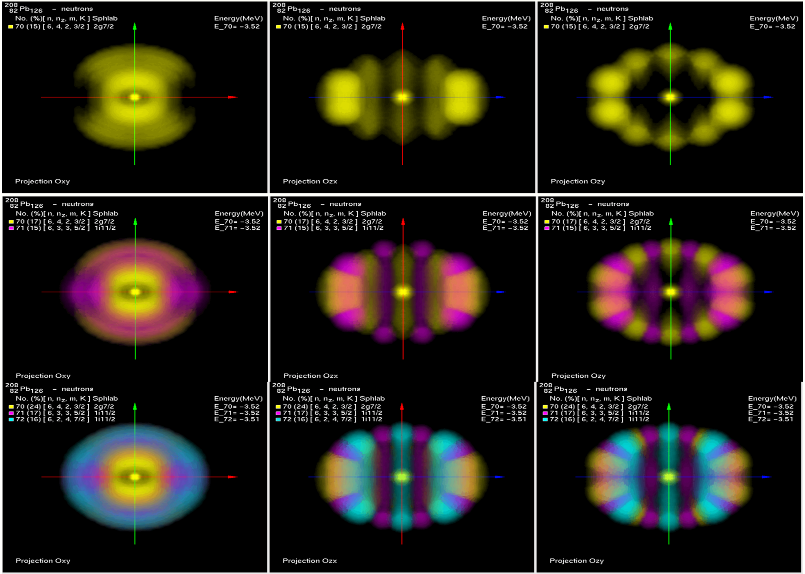

Concluding Observations and Suggestions

Concluding Observations and Suggestions

- **Programs realising certain options are being installed**

Concluding Observations and Suggestions

- **Programs realising certain options are being installed**
- **Please download the presentation to get accustomed**

Concluding Observations and Suggestions

- Programs realising certain options are being installed
- Please download the presentation to get accustomed
- If you have questions – you may contact us by email